Scaling Acoustic Directional Couplers using 3D Printing

A thesis

submitted in fulfillment

of the requirements for the degree

of

Masters of Engineering (Electronics)

at the

University of Waikato

by

M.S.G MacDonell

2015

Abstract

Acoustic directional couplers permit separation of forward and reverse sound pressure waves. This separation opens the way to traceable, precision acoustic reflection measurements. In order to span the audio spectrum, multiple couplers will be required as each coupler only operates slightly over one octave. To reach 20 kHz or above requires very small, mechanically-precise construction. We achieve this precision using 3D printing techniques.

The Lagasse design method was used by Pennington to create a coupler that operated over a designed range of 1–2 kHz. This design was scaled to create an acoustic directional coupler with a designed range of 10–20 kHz. Because frequency scales inversely with the size of the coupler, the coupler needs to be built with a very high degree of precision. The coupler was therefore designed and modeled in SolidWorks and 3D printed to high precision.

Characterization of the couplers was achieved using two distinct methods. The first, a preliminary measurement method to test the hypothesis and the second, a high precision automated measurement. The automation was scripted in python on a Ubuntu Linux distribution.

Future work may include an Acoustic coupler to be used in ultrasound, to do this the coupler would need to be scaled a further 2.5 times. This would likely prove difficult as the wavelengths at 50 kHz are in the order of mm, comparable with those of electromagnetic waves at 44 GHz.

Acknowledgements

Jonathan Scott, Kyle Pennington, Mark Jones, Scott & Vicki MacDonell.

Contents

Chapter 1

Introduction

Currently there are several tests for the measurement of the acoustical properties of materials [1] [2] [3]. One standard method is the "impedance tube method" [1]. This method uses a simplistic measurement of the standing wave in a tube to determine the impedance and absorption of a material. By building a tube with a load placed at one end and driven by a loudspeaker at the other a standing wave at a single frequency is created, a probe microphone is then slid along the tube to measure the standing wave [1]. All of these methodswork in a very similar way and these methods all suffer from poor calibration or great uncertainty in their results [4]. The measurements themselves may be precise but the difficulty in accurate measurements lies with other variables like room size, geometry and calibration. The spread of results using the same methods and materials is very large [5].

It is often assumed that a directional coupler is inherently an electromagnetic device, since the majority of commercial examples have either coaxial or electromagnetic waveguide ports. Nevertheless, acoustic directional couplers also exist. These are four port devices and behave much like a conventional directional coupler, except that the ports are acoustic waveguides that conduct pressure waves in a medium, typically air. The operation of an acoustic directional coupler is similar to that of a directional coupler in radio frequency (RF) circuits in that it is a four port device with reverse and forward coupled

ports. Generally a directional coupler is a four port network in which portions of the forward and reverse traveling waves on a transmission line are separately transmitted to two of its ports [6].

The Acoustic directional coupler has been described by P.Lagasse [7] and shown to work by K.Pennington [4] as a reflectometer in a single port vector network analyzer. To prove that frequency range scales with the size of the acoustic directional coupler, we built a coupler an order of magnitude smaller than that described by Pennington. We expect the frequency range to scale inversely i.e this scaled coupler is hoped to operate at frequencies ten times higher those of the coupler built by Pennington. The Coupler built and described by Pennington was designed for a frequency range of 1–2 kHz which had an actual range of 800–2200 Hz. Thus we expect our scaled coupler will also operate outside its intended range of 10–20 kHz.

There are two crucial aspects of an acoustic directional coupler that need to be considered and measured in order to characterise it and be confident in its operation. These are the acoustic loads and the directionality. The acoustic loads are largely responsible for the directionality of the coupler, they are analogous to the matched loads in an electromagnetic coupler. The acoustic loads therefore need to perform well in order for the overall coupler to perform well. Also to ensure measurement of the directionality is reliable, the sliding load method from [4] can be used. It is possible to calibrate for the load and infer the inherent directionality of the acoustic coupler using the sliding load method. We intend to use this sliding load method to determine a suitable load for the scaled coupler and infer the inherent directionality of the coupler.

The directionality of a coupler over its operational range is an important specification and this is the specification we are most concerned with. If directionality exceeds 6 dB then vector correction is possible [4]. We expect the directivity of our scaled couplers to easily exceed 6 dB and actually expect their measured directionality to be better than 15 dB.

In order to achieve our coupler, we needed to accurately produce waveguide

cavities with 6 mm square openings and branching networks to within strict tolerances. To construct our couplers with such precision we employed two different 3D printers. 3D printing is emerging as a cost effective construction and prototyping technique. 3D printing technology now has both a high end market and low end consumer market. This enables cost effective prototyping for businesses big and small. The 3D printers we chose are the Objet30 and MakerBot replicator, from the high and low end of the market respectively. They are distinctly different in their operation, material use, running costs and initial cost. We chose these printers in order to determine if the accuracy, precision and quality of the printed coupler would play a significant part in its overall performance.

The characterization and measurements of our scaled and 3D printed couplers was done with two distinct methods. A preliminary measurement and a high precision measurement. The preliminary measurement was made using commonly available bench equipment; an arbitrary waveform generator and oscilloscope. This preliminary measurement was used to quickly test our hypothesis. The high precision measurement was automated, scripted in python and utilized an Audiobox1818VSL audio interface to perform the measurement.

In order to create a measurement system that spanned the audible spectrum (20-20,000 Hz), a set of some 10 different-sized couplers would be required. Some applications would benefit from an instrument that reached or exceeded 50 kHz. For an Acoustic coupler to be used in this ultrasound range the coupler would need to be scaled a further 2.5 times. This may potentially prove difficult as he wavelengths at 50 kHz are comparable with those of electromagnetic waves at 44 GHz.

As Pennington effectively demonstrated, a single ported VNA can be made using an acoustic directional coupler. The calibration and vector correction techniques used in modern electromagnetic VNA's may in the future be extended to a dual-port acoustic VNA. Pennington expects applications and

commercial implications in the fields of architecture, biomedical diagnostics, sound reproduction, and agriculture [4]. It would seem logical that these fields would also thereby benefit from the development of a dual-port acoustic VNA.

The results of our investigation should firstly indicate if 3D printing is an appropriate construction method, secondly determine whether scaling a pre-dimensioned coupler is an effective method for creating couplers with a higher/lower frequency range and thirdly establish an effective acoustic load material for the upper half of the audible spectrum.

Chapter 2

Lagasse coupler design and application

2.1 Lagasse design

As one may expect, an acoustic coupler is a waveguide, and as such design can be approached in the same manner as a microwave waveguide [7]. Using this approach, Lagasse developed the acoustic directional coupler for use as an acoustic reflectometer, which enables swept frequency measurements of a materials reflection coefficient [7].

Lagasse described the acoustic directional coupler as a lossless four port network, with an associated S matrix. The matrix values are as follows:

1. a_1 is the incident wave at port 1.
2. b_1 is the outgoing wave at port 1.
3. C is the coupling coefficient.
4. $1/D$ is the directivity or directionality.
5. $Z = 1 - C^2 - K^2 - (C.D)^2$
6. K is the reflection coefficient at one port when all others are matched.

The standing wave ratio (SWR) is calculated as SWR $= (1 + K)/(1 - K)$. 'For an ideal directional coupler, D and K vanish, and C has a fixed value for all frequencies' [7]. The outgoing wave on each port b_1–b_4 are related to the inserted signals on a_1–a_4 by the S-matrix. This matrix ideally relates b_1 to a_3 by the coupling coefficient C and a_4 by $\sqrt{Z}$.

$$\begin{bmatrix} b_1 \\ b_2 \\ b_3 \\ b_4 \end{bmatrix} = \begin{bmatrix} K & C.D & C & \sqrt{Z} \\ C.D & K & \sqrt{Z} & C \\ C & \sqrt{Z} & K & C.D \\ \sqrt{Z} & C & C.D & K \end{bmatrix} \times \begin{bmatrix} a_1 \\ a_2 \\ a_3 \\ a_4 \end{bmatrix}$$

When the coupler is ideal D and K vanish so the s-matrix can be multiplied with D and K replaced with zero.

$$\begin{bmatrix} b_1 \\ b_2 \\ b_3 \\ b_4 \end{bmatrix} = \begin{bmatrix} 0 & 0 & C & \sqrt{Z} \\ 0 & 0 & \sqrt{Z} & C \\ C & \sqrt{Z} & 0 & 0 \\ \sqrt{Z} & C & 0 & 0 \end{bmatrix} \times \begin{bmatrix} a_1 \\ a_2 \\ a_3 \\ a_4 \end{bmatrix} = \begin{bmatrix} Ca_3 + \sqrt{Z}a_4 \\ \sqrt{Z}a_3 + Ca_4 \\ Ca_1 + \sqrt{Z}a_2 \\ \sqrt{Z}a_1 + Ca_2 \end{bmatrix}$$

When adapting existing microwave coupler designs, Lagasse asserts that the most suitable structure for an acoustic directional coupler is the branch-guide coupler. This design uses short lengths of waveguide between the two mainlines to achieve coupling. The branch-guide coupler also best satisfies the infinite wall stiffness associated with the Neumann boundary conditions. This is because we can create wall thickness' that are a non-negligible fraction of the wavelength [7]. The thickness of the walls in the branch-guide coupler not only contribute to the isolation between the two mainlines but also improves performance of the network because "the branch lines can be incorporated in the synthesis procedure" [7].

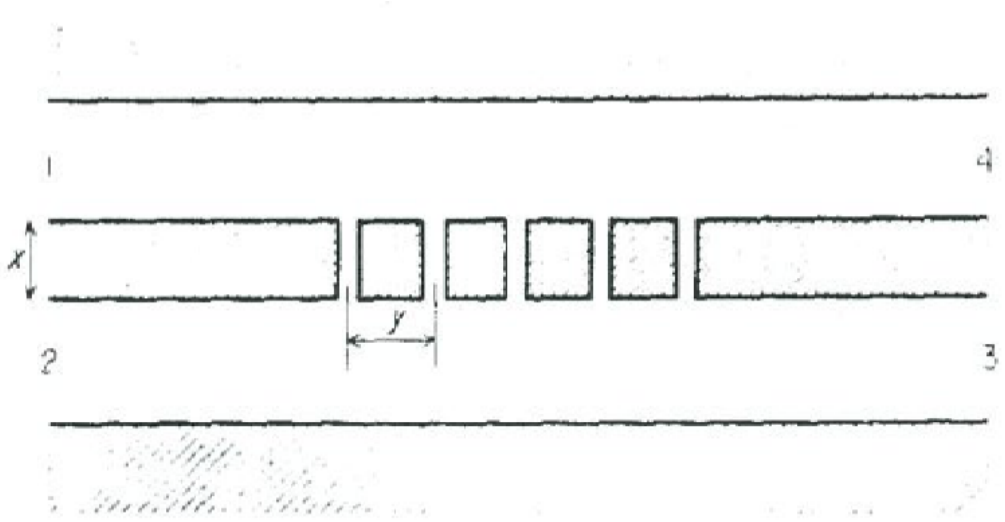

Figure 2.1: General shape of a branch guide coupler as drawn in [7].

$$f_c = c/2a \tag{2.1}$$

$$R_c = p_o c/S \tag{2.2}$$

In a square waveguide the first order mode has a cut-off frequency of f_c which can be calculated using equation 2.1 where c is the speed of sound and a is the side of the square [7]. The speed of sound in air has a dependence on temperature but is normally assumed to be negligible. The characteristic impedance of the fundamental mode in the guide (R_c) is inversely proportional to the 'surface of the cross section' (S) where $p_o c$ is the characteristic impedance of air[7]. Lagasse briefly discusses acoustic loads saying 'Cones in highly absorbing material provide good reflection free terminations, causing a SWR of less than 0.2 dB in the frequency range of interest'[7].

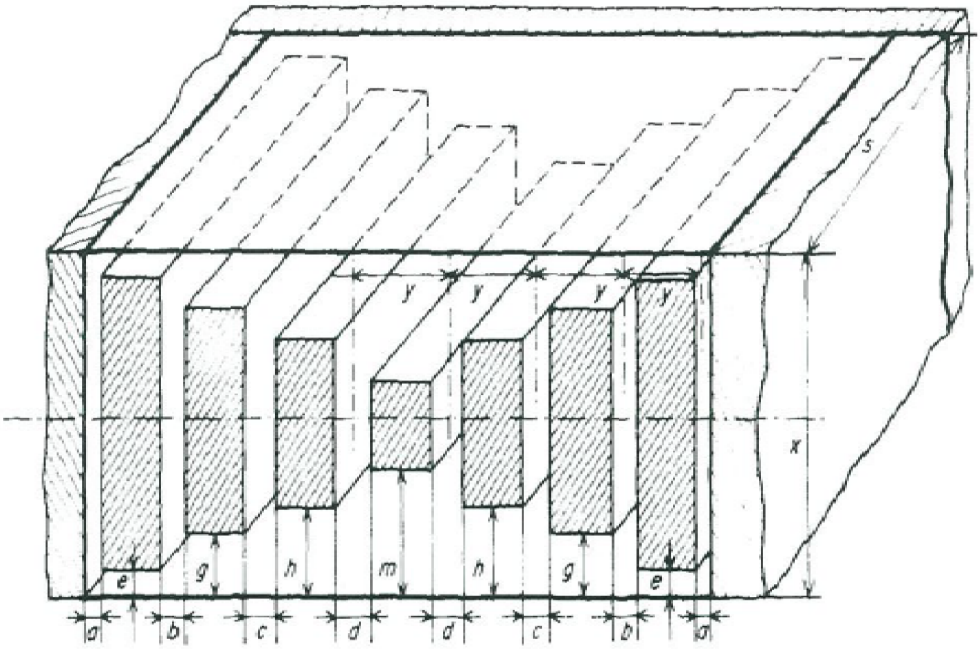

Figure 2.2: Isometric drawing of actual coupler shape and construction taken from [7].

The dimensions of the coupler built by Lagasse were decided upon by experimentation. First, by shunting the main line with a single stub, the relationship between the physical length and the electrical length of the stub was determined. These were then used to construct several narrow-band couplers for various ratios of x and y. This method provides the characteristic admittance and therefore the cross-sectional area of the branch and main guides [7]. The

dimensions x and y for a simple narrow band coupler are shown in figure 2.1 and the square waveguide minimizes the higher order effects [7]. The final coupler created was a wide-band eight-branch coupler [7]. The final structure by Lagasse had the following dimensions:

1. $a = 1.38\,\text{mm}$
2. $b = 3.41\,\text{mm}$
3. $c = 5.92\,\text{mm}$
4. $d = 7.75\,\text{mm}$
5. $x = 23\,\text{mm}$
6. $y = 29\,\text{mm}$
7. $e = 0.81\,\text{mm}$
8. $g = 2.82\,\text{mm}$
9. $h = 5.38\,\text{mm}$
10. $m = 6.61\,\text{mm}$
11. $S = 30\,\text{mm}$

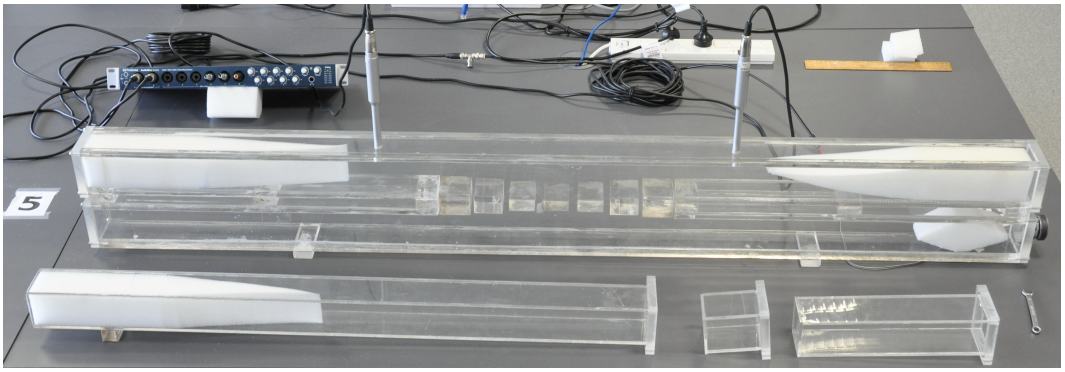

Figure 2.3: The Acoustic directional coupler built by Pennington, taken from [4].

Recently a version of the Lagasse design has been used to fabricate a single port vector network analyzer (VNA) [4]. The coupler used a 60 mm-square waveguide and had a design frequency range of 1–2 kHz and a usable range of 800–2,200 Hz. It was fabricated by welding sheets and machined blocks of acrylic material. Figure 2.4 shows a block diagram of the coupler used by Pennington [4]. A loudspeaker followed by a small pad introduces signal into port one. A matched load absorbs energy on port two. Ports 3 and 4 also have matching loads but each also has a microphone to sample the signal going

into the side load. In [4] it was shown that vector correction allowed precise measurements of acoustic S-parameters.

Using the dimensions that were used in [4] and scaling them we created our own coupler for use in another frequency range. By doing this our results are able to be directly compared with the results from [4].

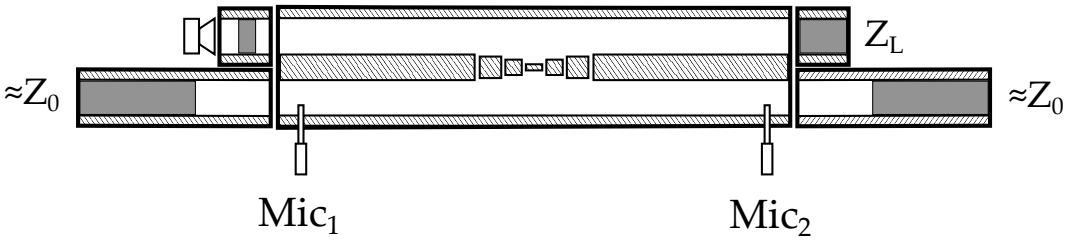

Figure 2.4: "Block diagram of the acoustic hardware. Microphones sense the sound pressure level in the two side arms of the coupler. The source is a small loudspeaker mounted behind an attenuating pad constructed of the same foam rubber used to make the loads"[4]. Z_L is the load material under test.

2.2 Applications and implications

The Directional coupler was used as a reflectometer by Lagasse [7] and later by Pennington [4]. A reflectometer is a directional coupler where the axillary line is matched at both ends i.e both the forward and reverse coupled ports have matched loads. A reflectometer is a crucial component in a modern vector network analyzer (VNA) or vector impedance meter (VIM) [4]. In a electromagnetic VIM or VNA a reflectometer replaces a slotted line waveguide used in older VNA techniques. It is not possible to construct a slotted wave-guide in a acoustic equivalent VNA because any breach in the wave guide radiates energy [4]. Pennington proposes calibration methods for an acoustic coupler using methods familiar from electromagnetic VNA calibration but uses a sliding load in the waveguide as a replacement for the open circuit standard [4], because an open circuit analogue does not exist in the acoustic case. This calibration process enables the coupler to be used as part of a 1-port acoustic VNA, as created by Pennington [4]. Pennington expects applications and commercial implications in the fields of architecture, biomedical diagnostics, sound reproduction, and agriculture [4].

Chapter 3

Design & 3D Printing

3.1 Design

The Lagasse design discussed in the last chapter and the dimensions from the coupler made by Pennington were used to create our own coupler. The dimensions for our coupler were scaled from Pennington's design and can be seen in Figure 3.1. Figure 3.1 was drawn in AutoCAD, a computer aided design (CAD) software package. We later used SolidWorks for our 3D CAD design.

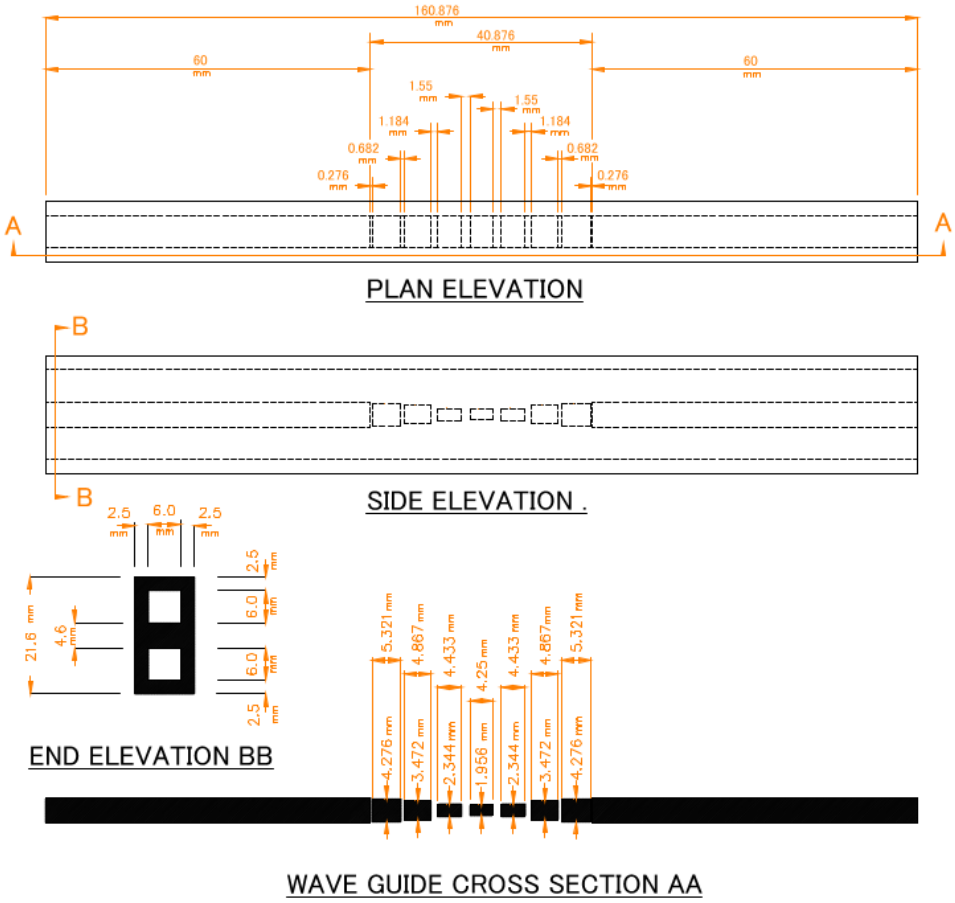

Figure 3.1: Plan, side and cross sectional elevations of the acoustic directional coupler as drawn in AutoCAD.

The cross sections AA and BB in Figure 3.1 show clearly the internal branch-guide structure and the waveguide openings respectively. The Waveguide openings on our scaled coupler are 6 mm by 6 mm square.

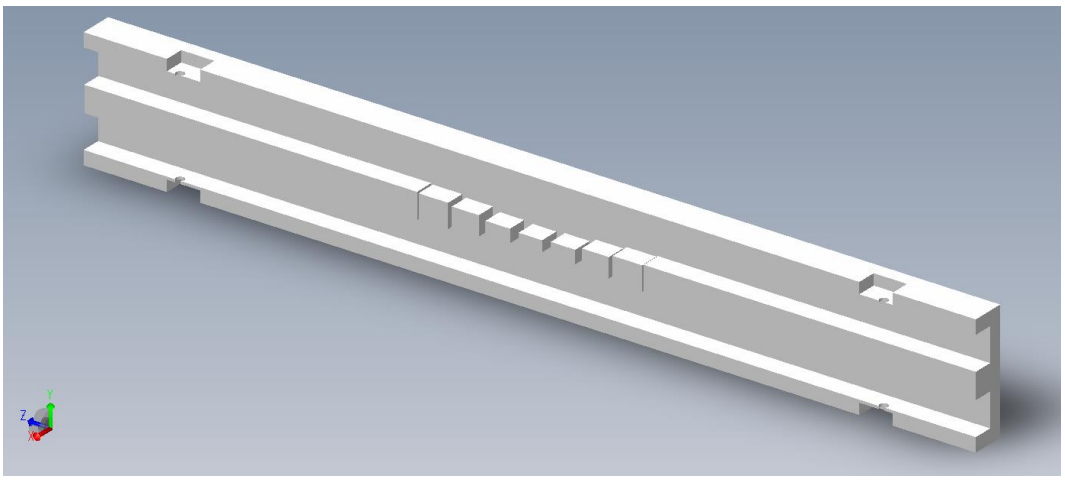

Figure 3.2: A cross-sectional view of the SolidWorks model for the scaled acoustic directional coupler.

We created a three dimensional model of this coupler design in SolidWorks. In the SolidWorks model we added side-ports for the placement of MEMS (micro electromechanical systems) microphones, these ports can be seen in a cross-section graphic view in Figure 3.2. This figure also allows us to see the internal geometry of the waveguides. Before printing we converted the design from the SolidWorks .SLDPRT file type to a .STL file which is a more commonly accepted file type for 3D printing. We built two versions, 3D-printed on different printers. One printer, was a MakerBot Replicator 2X and the other, an Objet30.

By printing our coupler using two different printers, we wish to determine if resolution, construction method or material have an effect on the performance of the coupler, but more specifically the directionality.

3.2 3D printing

3.2.1 MakerBot

The MakerBot 3D printer is an inexpensive 3D printer that is widely available, it uses an ABS filament which is an inexpensive stock material. It claims a layer resolution of 200 microns [0.0078 inches], and an X-Y resolution of 11 microns. The MakerBot melts the ABS filament and prints cross-hatched strands to make the layers of the part. Using this process it took approximately two hours and a few dollars worth of stock to build our coupler.

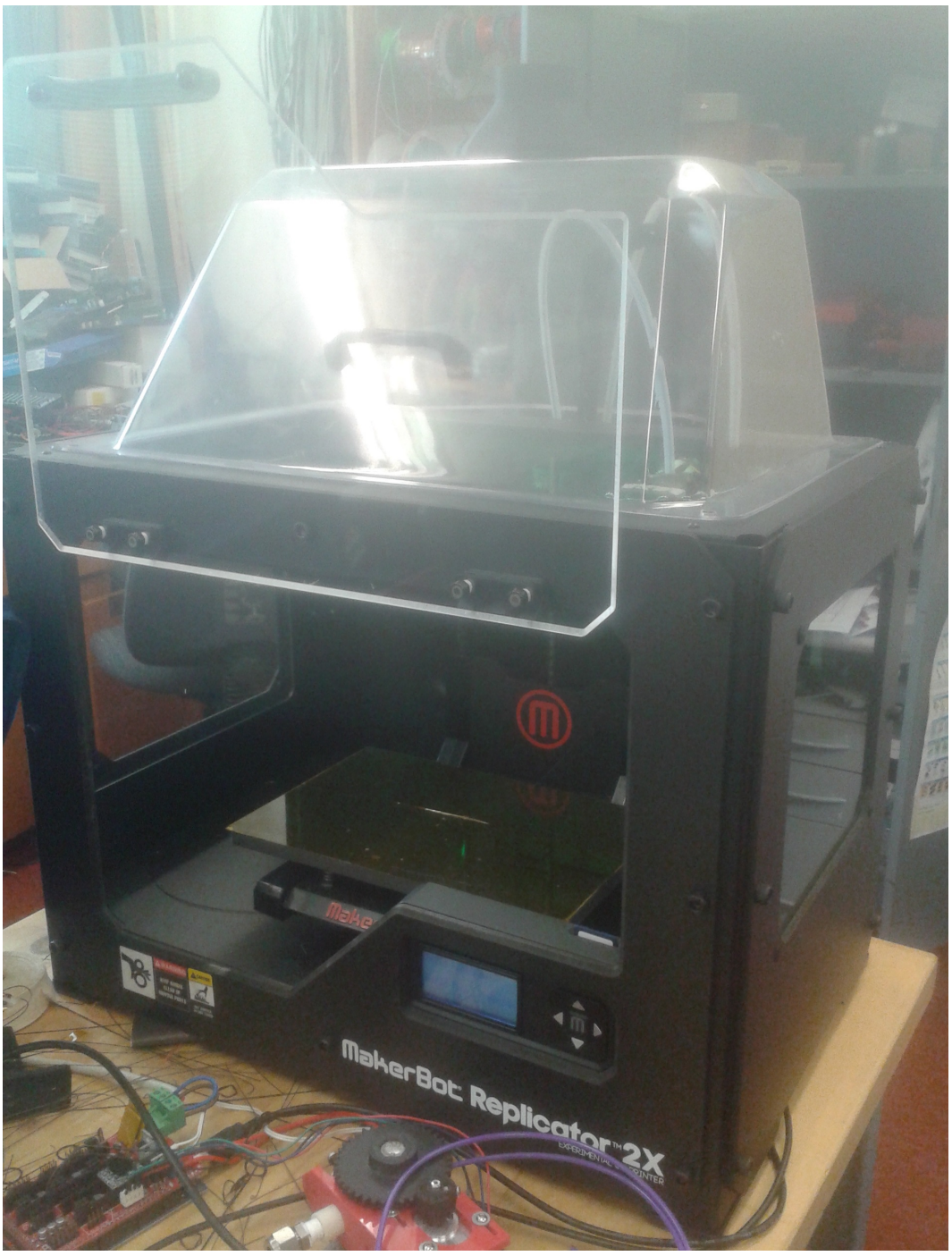

Figure 3.3: The MakerBot Replicator 2x.

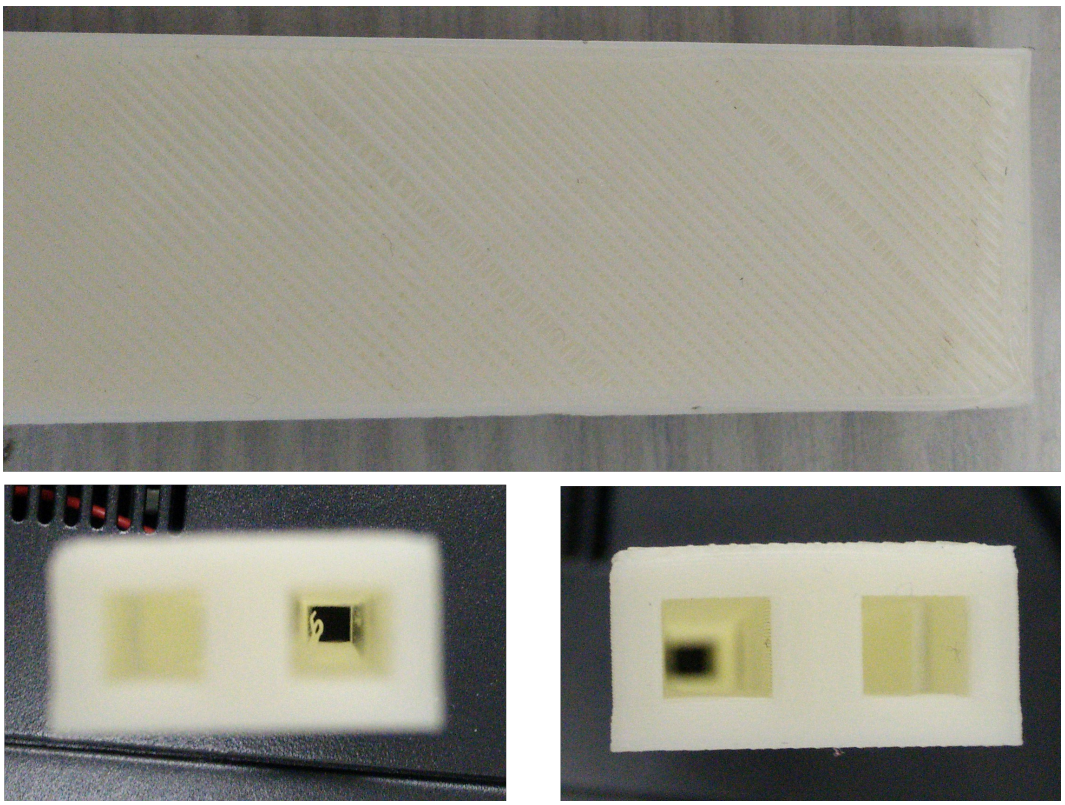

Figure 3.4: MakeBot coupler surface finish (Top) and collapsed plastic (Bottom Left).

The MakeBot printer created a coupler with a noticeable grain from its crosshatched layering process. The structure also had collapsed portions in the waveguide, the collapsed portions left the surface finish damaged and the collapsed plastic had to be cleared from the waveguide before experiments could be started. The MakeBot coupler was also slightly warped and shrank by approx 2 mm from the cooling of the plastic which affected its overall dimensional accuracy. These defects can be seen in Figure 3.4.

Figure 3.5: MakeBot coupler cross section.

A second coupler was made using this same printer for the sake of a physical cross-section which can be seen in Figure 3.5. This second print was cut using a band saw, the cut runs through the center of both mainline wave-guides. This cross section cut exposes both the top and bottom surfaces of the mainline waveguides as well as the branch-guide structure. Once this cut was made any melted material from cutting was carefully removed so that only the defects from printing are shown. This cut down the center of the coupler reveals the extent of the surface damage in the collapsed portions of the mainline waveguides which can clearly be seen, as well as an exaggerated cross-hatch pattern. The cross-section also reveals that the dimensional accuracy has a potential to distort the branch-guide structure in the coupler, so that walls touch and are not square.

3.2.2 Objet30

Figure 3.6: The Objet30 Printer.

The Objet30 is a comparatively more expensive printer, and uses a resin to create the layers of the main structure. It also prints a 3D honeycomb wax support structure alternately layer by layer. The Objet30 claims a resolution and layer thickness of 28 microns and an accuracy of 100 microns [0.0039 inches]. The resin is stored as a powder which is then heated and dissolved to travel to the printing head. The resin is printed as a layer to form the main structure which is then cured with ultra-violet (UV) light. The support structure layer is then printed to encase the part and fill any voids within the part. The support structure must be removed after the part is completed. This is done with a dilute sodium hydroxide (NaOH) solution.

Figure 3.7: The Objet30 coupler surface.

The support structure prevented the collapse of the waveguides and the resin layers bonded together to give a very smooth surface finish. This surface finish is maintained inside the waveguides because of the support structure preventing collapse. This printer also creates parts with greater dimensional accuracy because they do not warp or shrink as each layer is cured and cooled as it is printed.

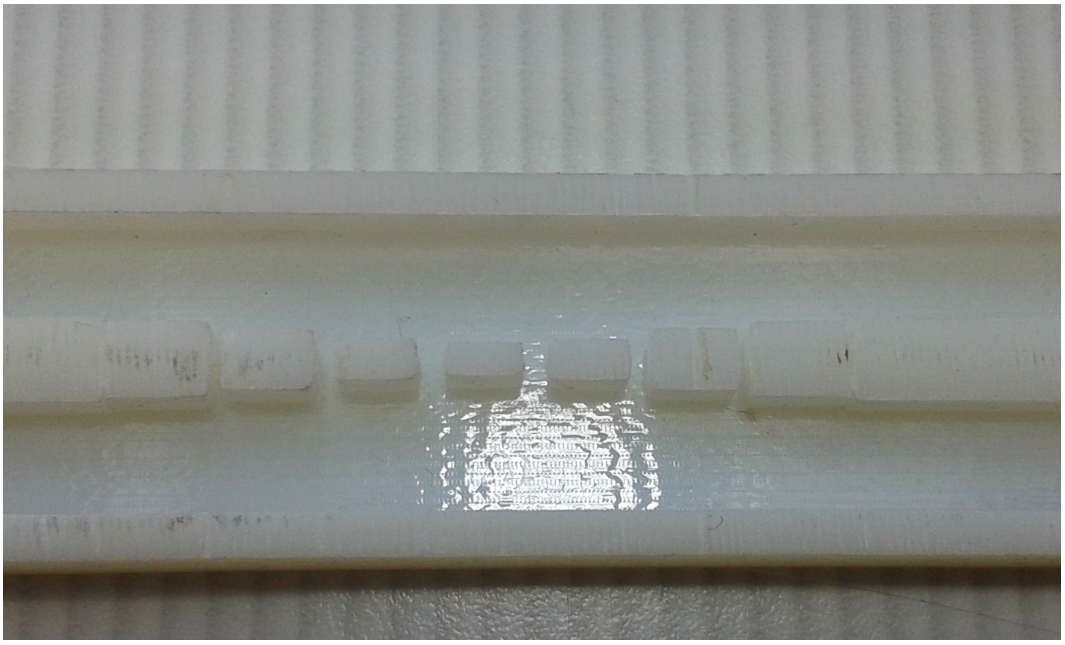

Figure 3.8: Objet30 coupler cross section.

In Figure 3.8 we can see the mainline waveguide and branch waveguide structure in the Objet30 printed coupler. The surface finish and dimensional accuracy can be seen, and are much better than that of the MakerBot coupler.

Having printed two couplers of different quality we need to test their performance. In the next chapter we develop a test method and discuss acoustic loads, which are required in order to terminate the coupler ports.

Chapter 4

Acoustic loads, Directionality and Measurement

In the previous chapter we presented our 3D printed couplers. In order to test these couplers effective acoustic loads are needed, and a test method. Lagasse in his paper brushed over how important a good acoustic load is, and did not present how to select a "highly absorbing material".

As discussed in the introduction, there are several tests for the measurement of the acoustical properties of materials [1] [2] [3], and that these methods have been shown to suffer from inaccuracy. A material with a high adsorption coefficient for our loads is required. Knowing that our current industry standard test methods are reasonably poor we chose to use the sliding load method presented by Pennington, to select our loads [4].

4.1 Sliding load test

The sliding load test method, measures the effectiveness of a material as a load directly. First by terminating the coupled and reverse coupled ports and then, with the same material sliding along the mainline, the phase of the reflections can be changed. This change in phase can be measured directly as an amplitude change on the coupled port.

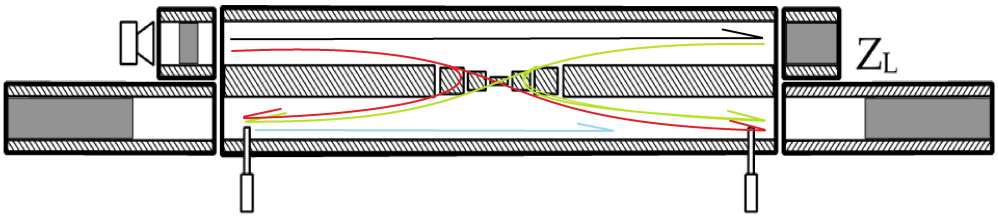

Figure 4.1: Graphic presentation of reflections.

In Figure 4.1 an experimental set-up can be seen. The black arrow is the main forward signal, the red is the fraction of forward signal to the coupled port. The green is the reflection from the load on the output port. The green and red signals can potentially be reverse coupled, and this is shown with the secondary arrows through the coupler. The blue line is the secondary reflection from the load at the decoupled port. The reverse coupled signals and secondary reflections are non-ideal phenomenon and the directionality of the coupler is dependent on these non-ideal components being negligibly small.

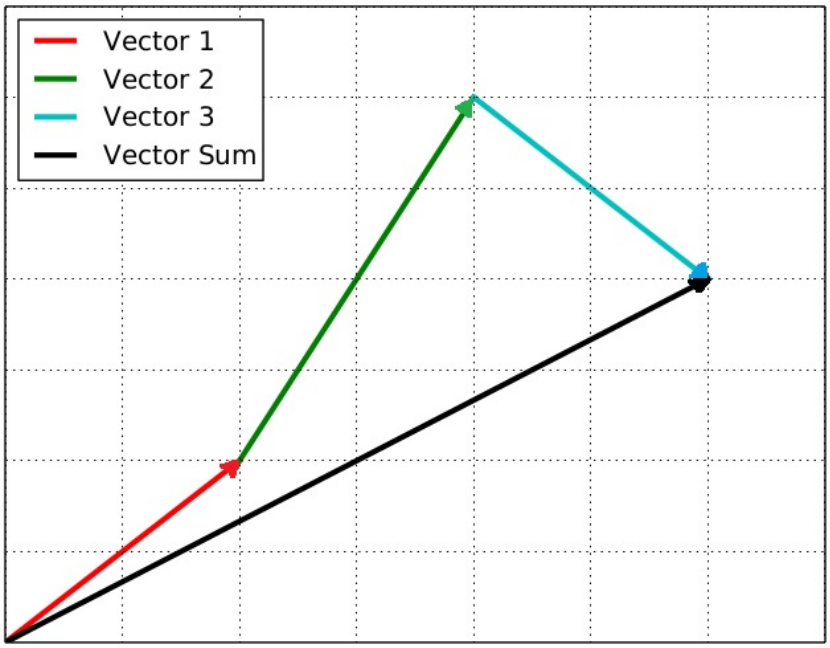

Figure 4.2: The vector addition of non-ideal signals at the coupled port. NB: This representation is purely for the purpose of explanation

Directionality is measured between the coupled and decoupled ports. Directionality is defined as $10log(P_c/P_d)$ where P_c is the power at the forward coupled port and P_d is the power at the reverse coupled port[6]. These ports are shown in Figure 4.1 as the two ports with microphones. Each of coloured arrows in Figure 4.1 represents a signal or reflection in the directional coupler and corresponds to the same coloured vector in Figure 4.2.

The measured amplitude at the coupled port is the vector sum of all these components. As a load changes position, they change phase. If the the non-ideal components are small, the measured amplitude at the coupled port should not be seen much to change with the phase change due to load position. "An ideal load reflects none of the incident energy" [4]. This forms the basis for the sliding load test proposed by Pennington [4] as a method for determining the effectiveness of an acoustic load, and the inherent directionality of the coupler [4]. The output port load Z_L slides along the waveguide to change

the length of waveguide and thus the phase of the reflections. The vector sum is measured as the amplitude at the decoupled port and can be plotted on a smith chart. When measurements of the amplitude at the decoupled port for a sliding load are plotted on a smith chart, the radius of the fitted circle or spread of data represents the quality of the load, which ideally is a point on the smith chart. The position of the center of the circle indicates the quality of the coupler, an ideal coupler positions the center of the circle in the center of the smith chart [4].

Once an acceptable load is chosen, the directionality can be measured. This is done by measuring the amplitude at the forward and reverse coupled ports. If this directionality exceeds 6 dB the directional coupler is of sufficient quality for practical application.

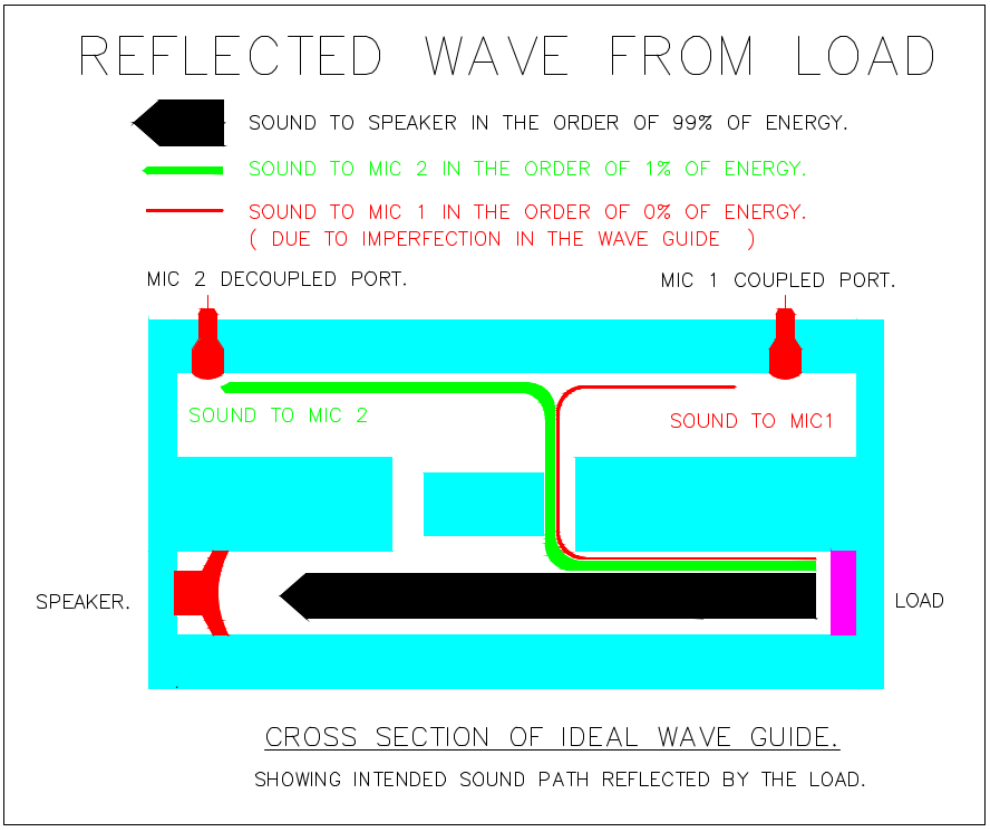

Figure 4.3: Reflections in coupler from load

Figure 4.3 shows the ideal and non-ideal signal portions from the reflected

wave off of the load. Ideally the amplitude of the reflection from the load is small, the signals are shown with thicknesses that represent their relative amplitude.

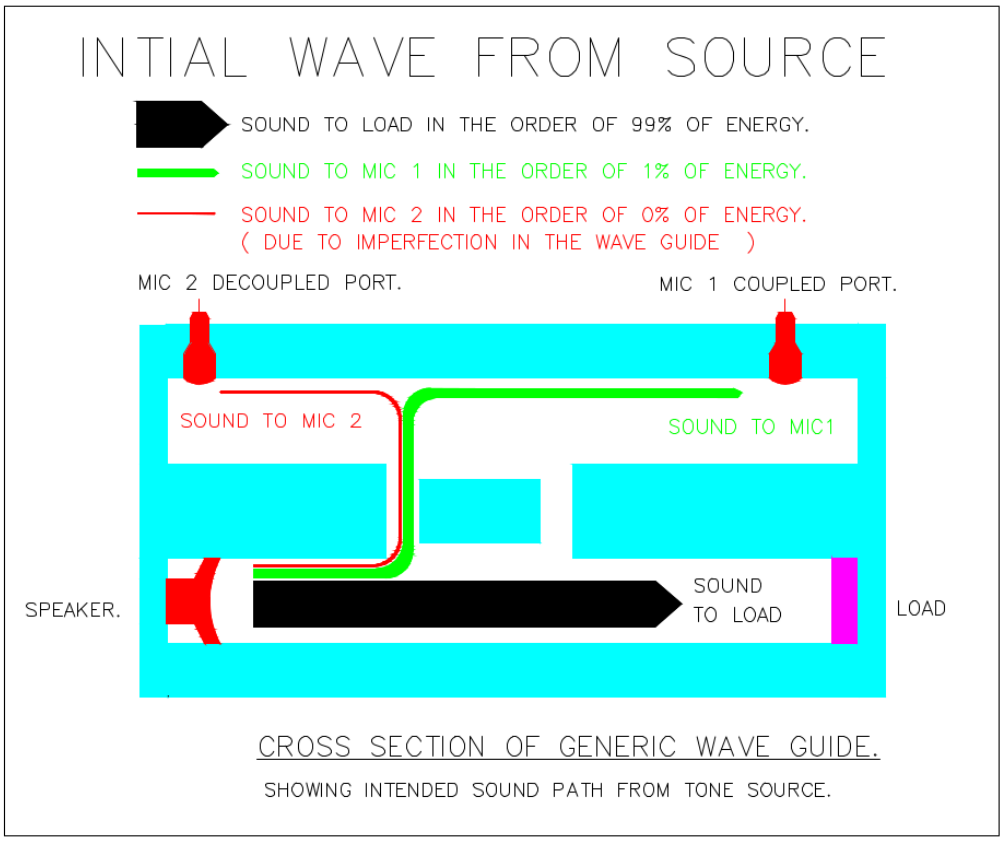

Figure 4.4: Injected signal in coupler

Figure 4.4 shows the ideal and non-ideal signal portions of the incident wave on the load. The two figures 4.3and 4.4 combined show how the forward and reverse coupled ports get their signal. As two separate figures, the signal paths are more easily seen and included for clarity.

Figure 4.5: Example earplugs: We used the foam type on the left hand side.

We chose earplugs as our loads for initial testing, earplugs have a typical attenuation of 40 dB up to 8 kHz [11]. This attenuation will include any loss due to reflections but it was assumed that earplugs could be an acceptable load and were used as our first test material. In the next chapter we begin to measure our couplers using a simple bench set-up of signal generators and oscilloscopes.

Chapter 5

Manual Methods and Measurements

The previous chapter stressed the importance of the acoustic loads. This chapter addresses the measurement of our loads, and then the measurement of the directionality. A simple bench set up was created in order to do obtain these preliminary results. Later a fully automated measurement method was realised. A diagram of the bench set up including electrical connections can be seen in Figure 5.1. The bench setup consisted of an oscilloscope, function generator and stereo amplifier. To see the set-up diagram in full detail please see the pullout A2 drawing (1 of 2).

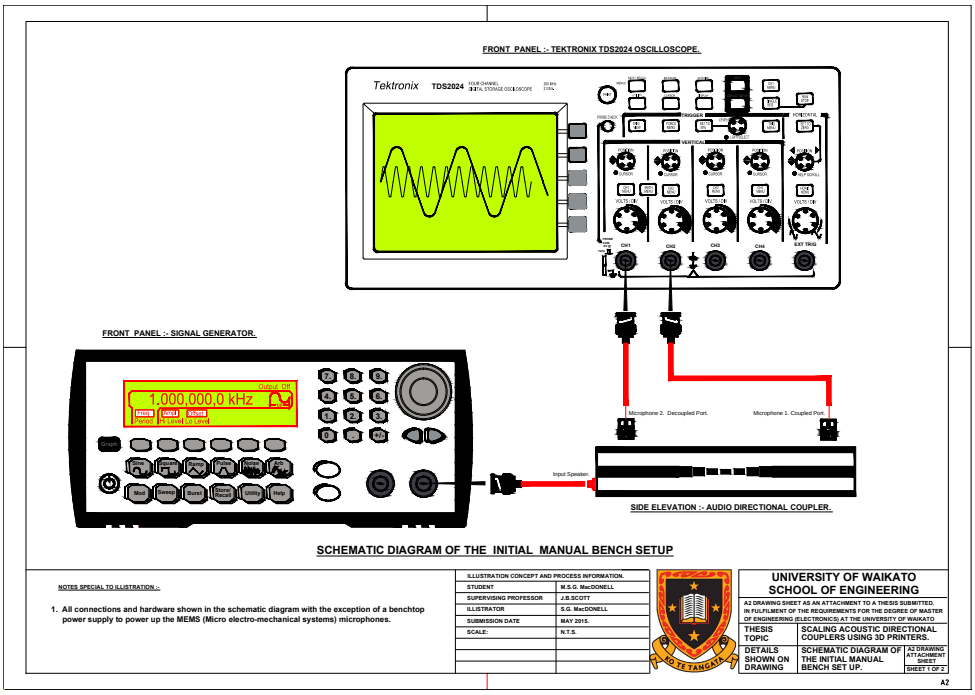

Figure 5.1: Bench setup diagram.

By experimentation, it was found that sound leaking from the two unused microphone ports, significantly worsened the measured directionality. This was expected and these ports were filled with Blutack to negate this effect. Blutack was also used to seal our microphones and secure them in place. For our experiments yellow earplugs were used as acoustic loads on three of the coupler's four ports. Two MEMS microphones attached to the coupler and sealed in the designed ports, were used to detect the tone amplitude through a Tektronix TDS2014C oscilloscope. The MEMS microphones are powered at 3 V from a bench power supply. The experimental set up can be seen as used in Figure 5.2.

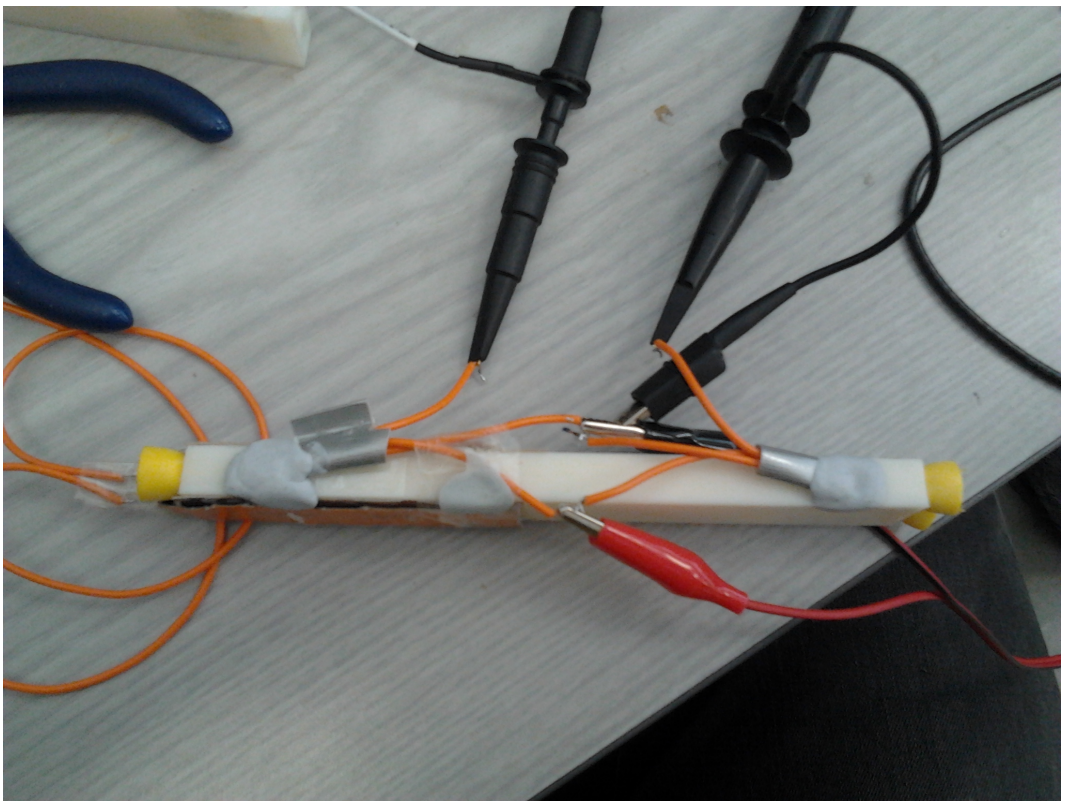

Figure 5.2: Coupler experimental set up. Earplugs can be seen as the yellow foam inserted at the ends. Microphones are sealed into the top of the coupler with Blutack™

In order to test the coupler we put a swept audio signal into port one with a matched load on port two. Ideally we would see a strong signal on the coupled port and a much smaller signal on the decoupled port.

5.1 Sliding Load

To ascertain what materials would be appropriate as acoustic loads the sliding method from [4] was used. The sliding load test was done manually by placing a load at one of the three positions and observing and noting the amplitude for two frequencies on an oscilloscope before repositioning the load. This method produced promising results, the amplitude did not visibly change on the oscilloscope trace for any position.

The acoustic loads used in the coupler are an important aspect of its performance and once we were satisfied with ear-plugs as loads we measured the directionality.

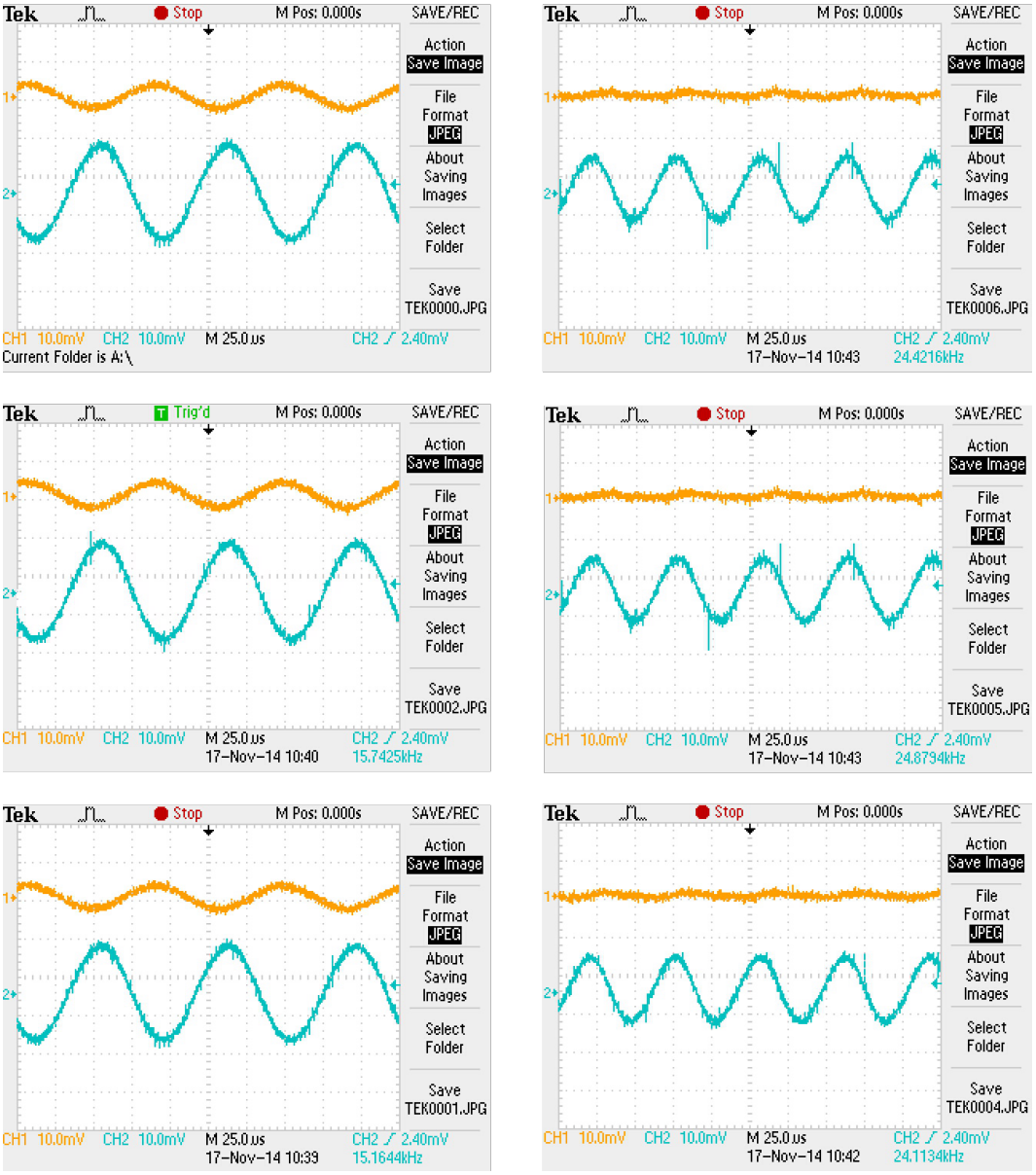

Figure 5.3: The scope traces for the load at three positions for two frequencies, 12 kHz and 18 kHz

The left hand column in figure 5.3 displays the oscilloscope traces for three load positions at 12 kHz and the right hand column shows scope traces for the same positions at 18 kHz. The larger blue signal is the forward coupled port in both instances, and the yellow trace is the reverse coupled port. These traces show that the amplitude is unchanged by load position, suggesting that the earplugs are in fact a reasonably good load material.

5.2 MakeBot Coupler

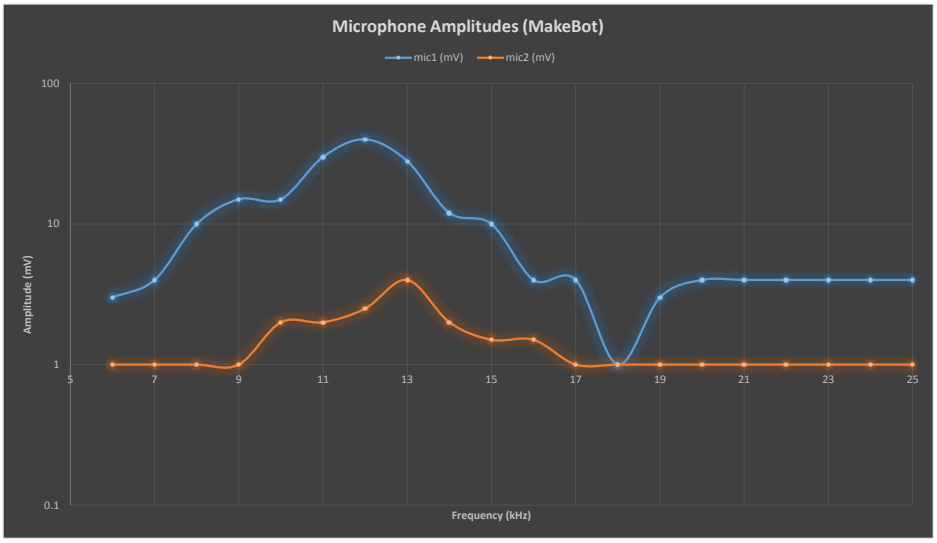

Figure 5.4: The lower resolution print port amplitudes.

Figure 5.4 shows the result of the measurement for the MakerBot print. The amplitudes in the MakeBot acoustic coupler were measured as voltage signals from the microphones. We are most interested in the ratio of the coupled to decoupled port signals, the directionality of the coupler. Directionality is plotted in figure 5.5.

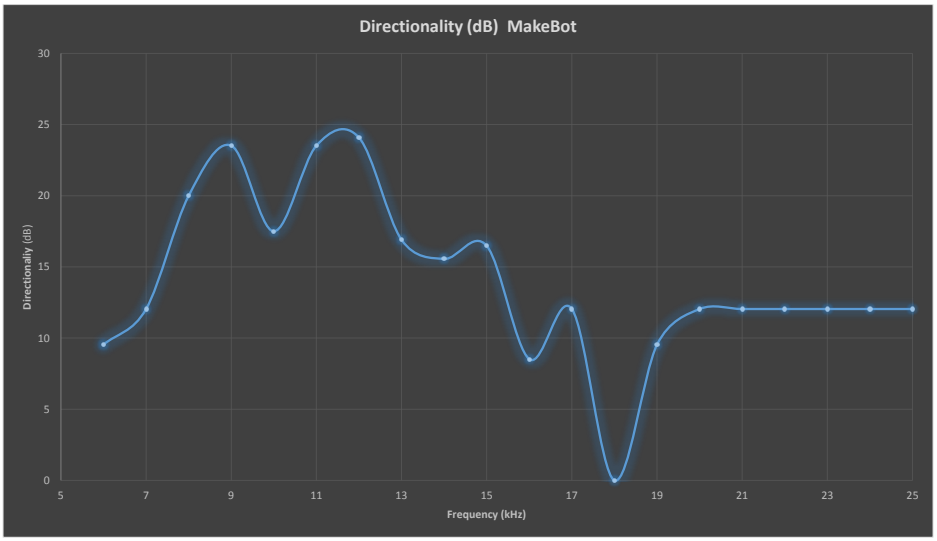

Figure 5.5: The lower resolution print directionality.

Directionality for both printed couplers was expected to be better than 20 dB from 10 kHz to 20 kHz, falling away around 7.5 kHz and 22.5 kHz. Directionality in the MakerBot print is excellent from below 10 kHz to at least 15 kHz, but it falters at some frequencies beyond this. The MakeBot coupler demonstrated apparently excellent performance but not over the expected frequency range. The directionality was better than 15 dB from 6 kHz to 15 kHz, but disappeared completely at around 18 kHz. The transducer used was a high frequency driver, because of this its frequency response prevented measurement at frequencies lower than 6 kHz.

5.3 Objet30 Coupler

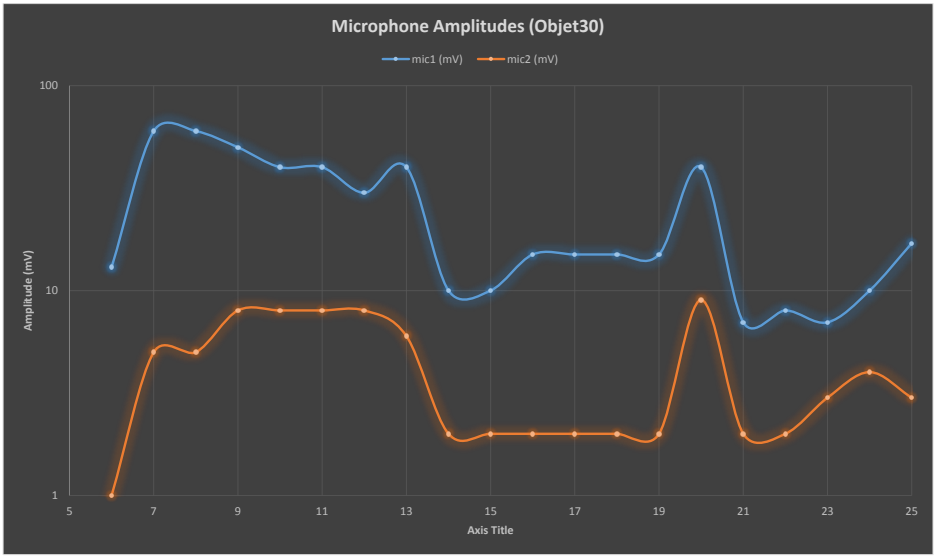

Figure 5.6: Amplitudes on the Coupled and decoupled port of the Objet30 print.

Figure 5.6 shows the result of the measurement for the Objet30 print. The amplitudes were again measured as voltage signals from the microphones and the directionality was calculated and plotted in Figure 5.7.

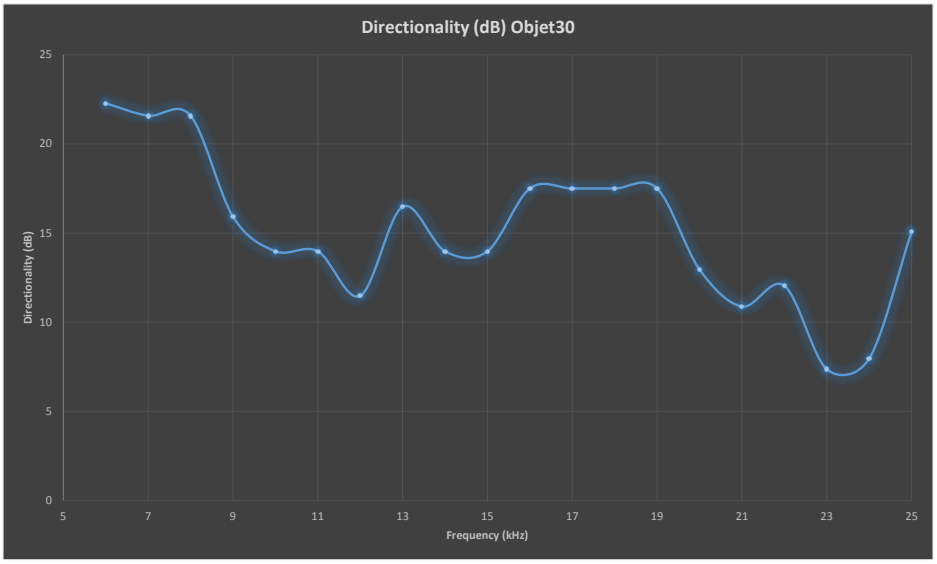

Figure 5.7: Acoustic coupler directionality averages 15 dB over the expected usable frequency range.

The Objet30 demonstrated superior performance, directionality was very much as predicted. The Objet30's directionality measured better than 15 dB for its entire expected range and extended to slightly higher frequency as well.

5.4 Bench Measurement Conclusions

Both of the measured acoustic couplers displayed excellent directionality. However only the Objet30 version behaved as expected with a range of 7–22 kHz. The MakeBot coupler displayed its directionality over a lower frequency band, approximately 7–15 kHz. The altered characteristics of the MakeBot coupler we believe can be attributed to the decreased resolution of the printer and the absence of a support structure. The resolution and shrinking of the printed coupler led to less accurate recreation of the internal geometry. The absence of an internal support structure while printing caused the walls of the mainline waveguides to collapse. The damaged surface and excess plastic left in the waveguide of the coupler causing a change to its behavior.

The Objet30 coupler did not suffer any of the issues affecting the MakerBot coupler. Its printing process with UV curing of each layer and support structure, lead to a higher quality print and ultimately a superior acoustic directional coupler.

In the next chapter we re-measure the performance of the Objet30 coupler using a more sophisticated method which will more accurately measure the loads and directionality of the coupler.

Chapter 6

Python, Hardware and Automated Measurements

The previous chapter presented preliminary measurements of both 3D printed couplers. Knowing the Objet30 printed coupler performs better than the MakerBot version, we now re-measure the Objet30 coupler only.

6.1 Hardware

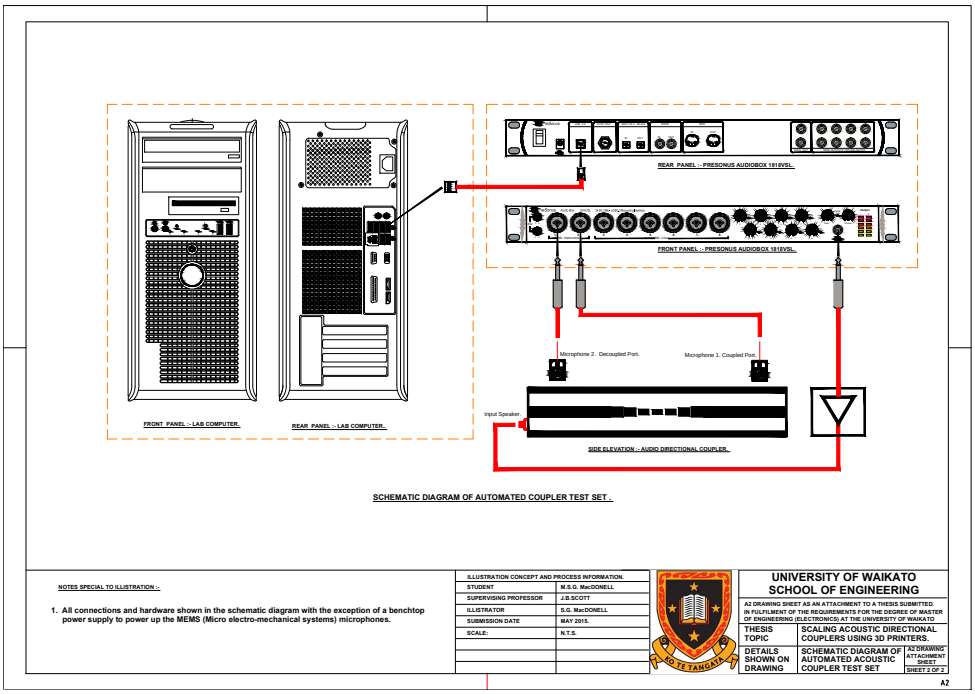

Figure 6.1: Automated measurement setup diagram.

The set-up of the equipment used can be seen in Figure 6.1. This Figure shows electrical signal connections between equipment. The Presonus audiobox1818 was configured as an external USB sound card to the Dell Optiplex750 and Python scripts automated data acquisition and processing. The Python scripts were written so that experiment run times could be kept to a minimum and that data was preserved for later processing. To see the set-up diagram in full detail please see the pullout A2 drawing (2 of 2).

6.2 Python Controlled measurements

The process of creating an automated and high precision method for measuring coupler directionality started by experimenting with scripts and software using the large acoustic coupler made by Pennington as the initial test coupler [4]. The choice to use a Linux Distribution was made because of the ready and free access to software. The AudioBox had to be set up in the Advanced Linux Audio Architecture so that it would function. Initially playback of tones and recording from the microphones was done with a piece of software called Audacity which is a digital audio workstation (DAW). Audacity would store all of the audio data as wave (.wav) files. This was not ideal for post processing of the captured information because of the tricky conversions required, made worse by the fact that wave files are a lossless audio format and tend towards large file sizes. Large file sizes were not desirable as folders can contain up to 150 files for a single swept measurement.

The block of python code in Listing 2 in the appendix is the frequency generator and initialization of capture using the Presonus AudioBox1818 for the automated measurement script. This script declares 8 channels of data, a sampling frequency of 96 kHz and a period size of 16. In the advanced Linux sound architecture (ALSA), this period size is the number of frames per write. The sampling frequency cannot be altered if using the AudioBox hardware.

The block of python code in Listing 1 in the appendix uses the initialized tone generator to play audio tones through the AudioBox output and to capture data using its inputs. The AudioBox hardware uses a sampling frequency of 96 kHz and this not changeable in software therefore all of the signal capture and processing is done with this sampling frequency. The code in Listing 1 also features a looping method so that multiple measurements can made consecutively with the data for each measurement placed into it's own directory for later processing.

6.3 Python signal processing and results

The python method for later signal processing is a reasonably large script that could easily be improved but however works for our applications. The script can be directed to process each measurement directory sequentially or to a specific directory. The script first reads a list of the files in the directory and steps over each file read it as an input. Using the "matplotlib" library the script plots the time domain information for both the forward and reverse coupled port. The script then uses a built in function of the "numpy" library to perform a fast Fourier transform (FFT). The output of the fast Fourier transform is then also plotted with the "matplotlib" library. By calling an external script written by Mark Jones, which in turn interfaces with a program written by Jonathan Scott, a discrete Fourier transform (DFT) is performed, and the output is written to a CSV file.

As a result of plotting the time and frequency domain signal as well as calling external scripts to perform DFT processing, this script takes some time to execute for small frequency steps. Because of this, it was debugged, using data from measurements using large steps of 500 Hz or 1 kHz which reduced the number of input files.

The output from the DFT which is written to a CSV is processed and plotted by another script.

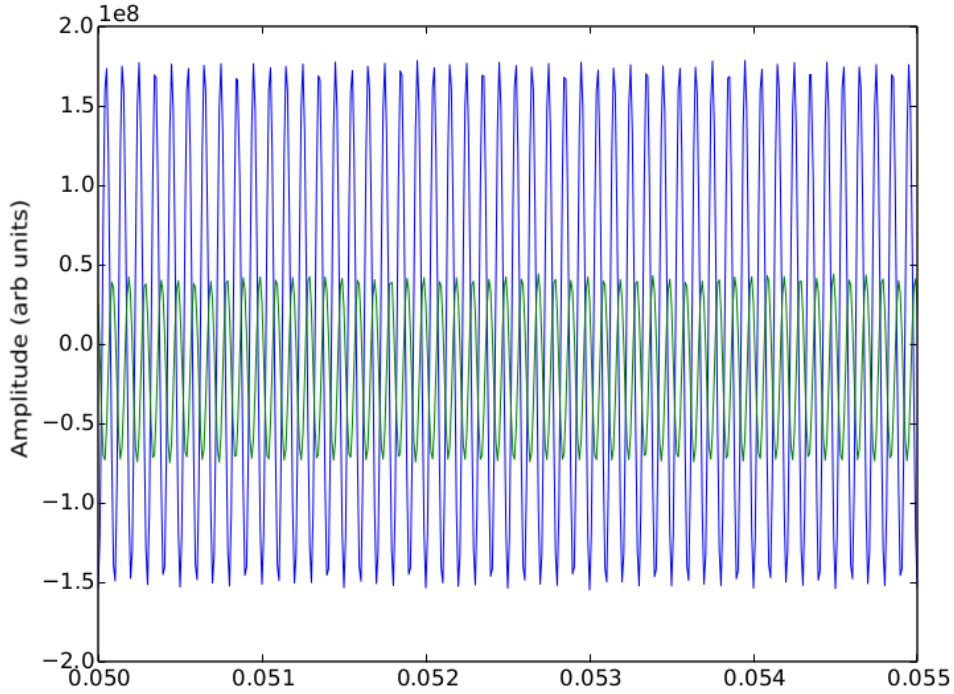

Figure 6.2: The time domain waveforms for the forward and reverse coupled ports at 10 kHz.

In Figure 6.2 the amplitude of the green trace (reverse coupled port) is clearly smaller than that of the blue trace (forward) which indicates that there is directionality for the coupler at this frequency. We apply a fast Fourier transform (FFT) to this data to acquire amplitude information, insure our noted frequency is correct and view the spectrum to observe noise and any harmonic content.

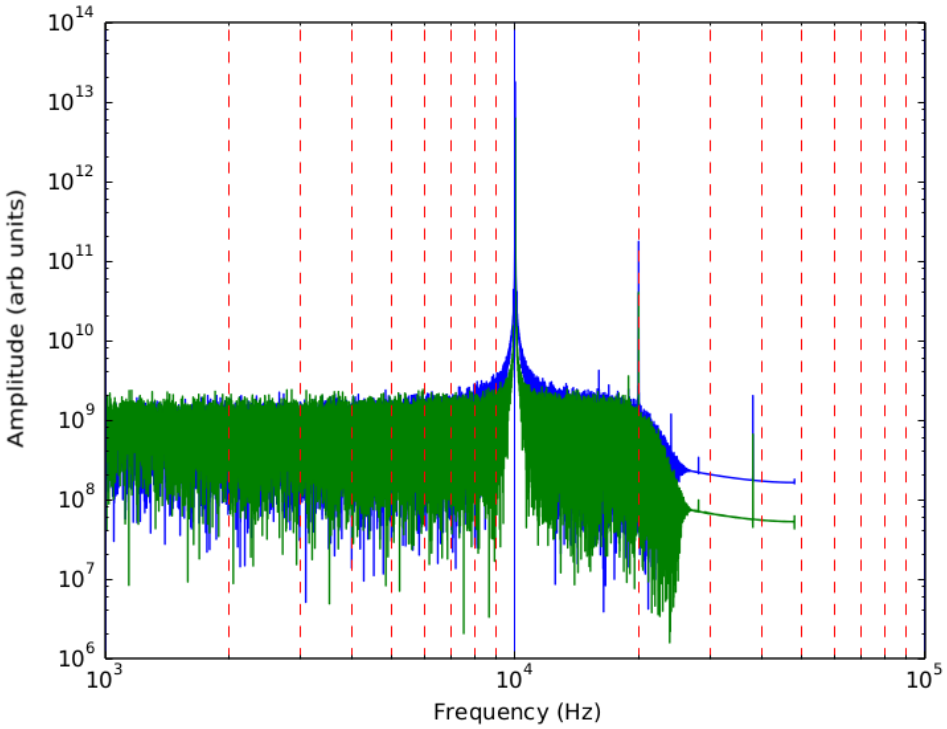

Figure 6.3: The FFT amplitude results for the forward and reverse coupled ports at 10 kHz.

The FFT results in Figure 6.3 show that for 10 kHz there is in fact some directionality because the blue FFT amplitude is larger than the green FFT amplitude. The signal is well above the noise floor and some harmonic content can be seen, this can be attributed to the non-ideal transducer and amplifier as they produce some unknown THD% that includes harmonics within the operational frequency range of the coupler, most notably the 2nd harmonic at 20 kHz. Our FFT results indicate that the measured frequency is what we expect i.e it is exactly the same as our injected signal and that there is directionality. The FFT is an excellent method for processing and producing spectra because it is computationally efficient, but in this case does not give amplitude to sufficient precision to reliably calculate directionality. In order to achieve sufficient precision with our data processing, we use a discrete Fourier transform (DFT), that given a frequency, calculates the amplitude for that frequency.

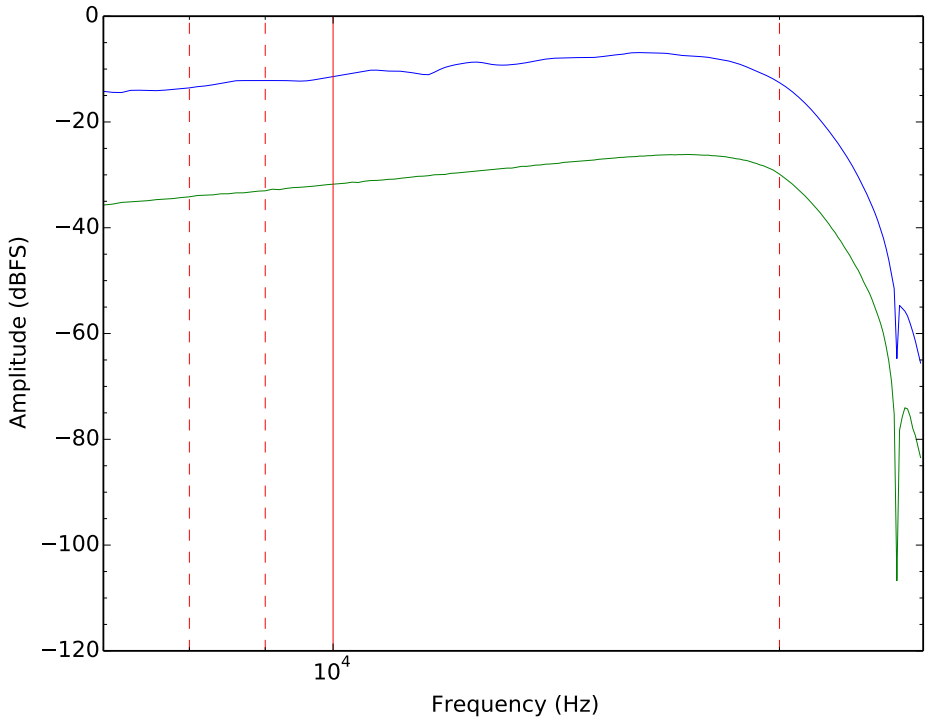

Figure 6.4: The DFT amplitude results from time-domain data.

The graph in Figure 6.4 displays the amplitude information obtained by the DFT for both the forward and reverse signal at each frequency. The Y-axis has units of "dBFS" this is not an SI unit but is common in digital signal processing (DSP) because of its convenience. It is a dB amplitude where the reference amplitude is the maximum possible amplitude for the data. In this case the maximum amplitude is $(2^24)/2$ because the data is formatted as signed 24 bit numbers. This shows clearly that the frequency range of the coupler extends past our designed upper limit of 20 kHz up to approximately 22 kHz. Measurement beyond this is not possible with the AudioBox hardware, because of the preamplifier specifications [8]. The low frequency extension however looks to extend past 7 kHz.

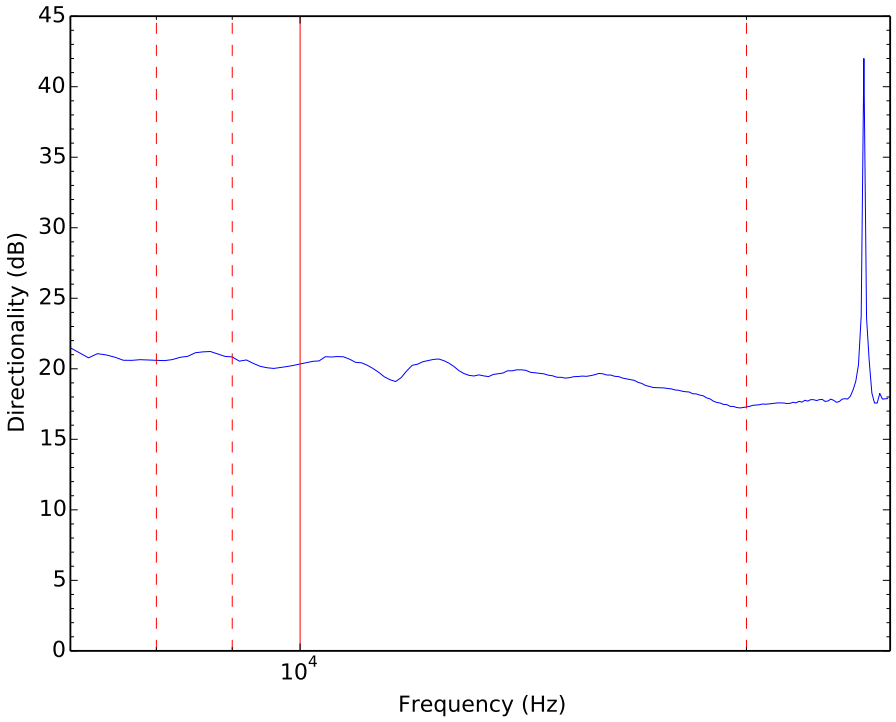

Figure 6.5: The directionality of the Objet30 coupler as calculated using the DFT data.

Figure 6.5 shows that the directionality is essentially constant with frequency. This is a slightly better and different result compared to our bench measurements. The directionality of the coupler here is calculated as approximately 5 dB better than calculated with the bench measurements on average. The difference we attribute to the inaccuracy of the data collected from the oscilloscope, this inaccuracy resulted from human error in reading data from the display. The directionality values beyond 22 kHz become less credible because the Presonus AudioBox preamplifier's have a frequency response of 20 Hz–22 kHz [8]. Beyond 22 kHz the sample rate of 96 kHz would support data up to Nyquist of 48 kHz without aliasing if the preamplifier's have an identical frequency response. However the results Show a large spike in directionality beyond 22 kHz which is probably due to some non identical frequency response in the preamplifier's.

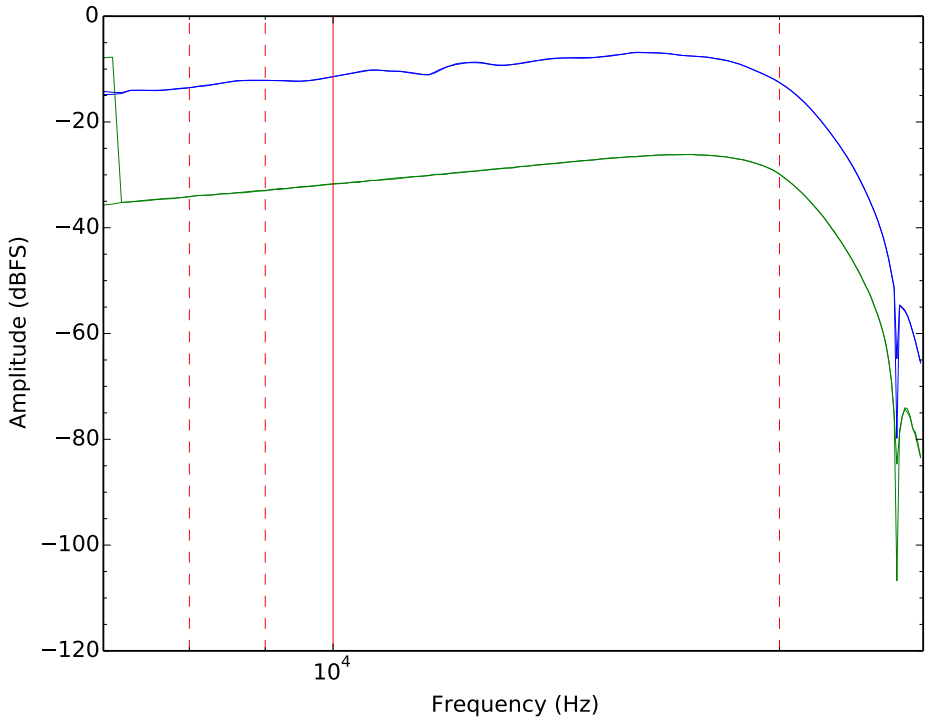

Figure 6.6: Amplitudes of our Objet30 coupler at two different load positions.

The Figure 6.6 is DFT amplitude data taken for two different load positions, the data is very close with little variation. This small variation in amplitude means that there are only small phase shifts in the reflections due to the load position. The small amplitude change with position and directionality being consistently well above 6 dB mean that the load imperfections can be corrected for.

The large variation seen in the second overlaid trace is due to the disturbance of moving the load, which in this case may have caused leakage or another phenomenon.

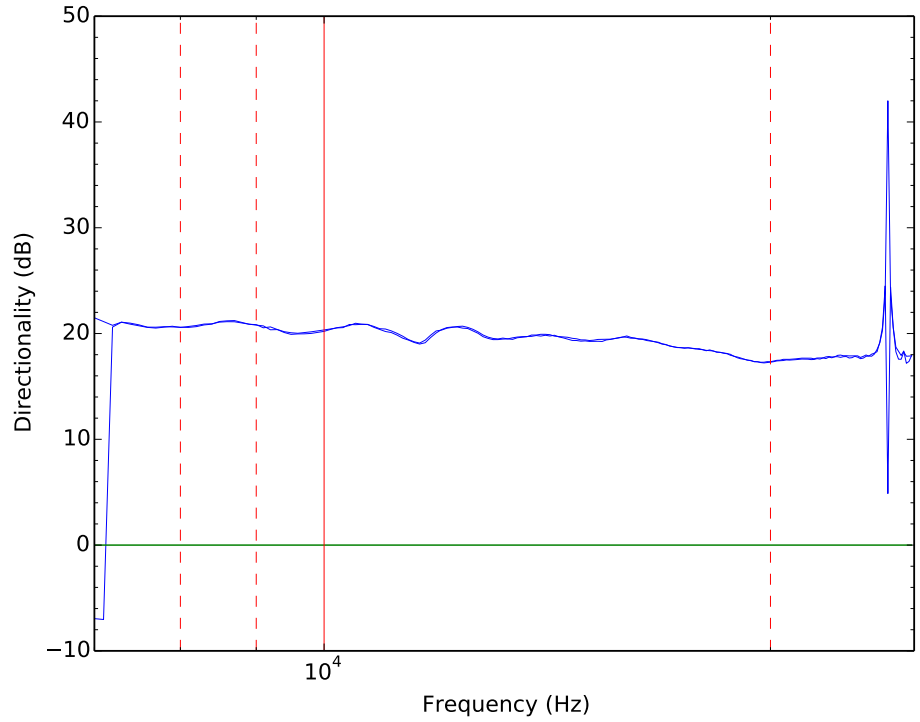

Figure 6.7: Directionality of our Objet30 coupler for two different load positions.

The Figure 6.7 is the directionality for the two load positions, the directionality is unaffected by the load position. The spike in directionality is present for both load positions beyond 22 kHz but spikes positively for one position and negatively for the other.

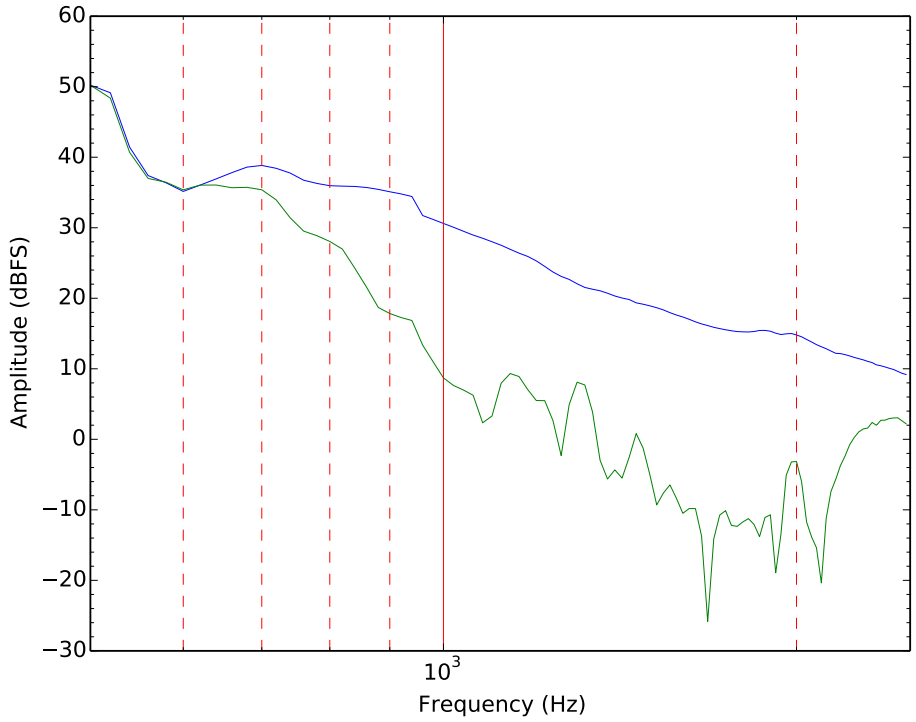

Figure 6.8: The DFT results for Pennington's coupler.

The Large lower frequency coupler built by Pennington, was measured using the same scripts and methods used to measure the 3D printed coupler but we used different microphones (Behringer ECM8000), powered by the AudioBox phantom power. The directionality measured in this large coupler was less consistent than that of the 3D printed coupler. We attribute this lesser performance to its construction. Because it was built from multiple parts, it is perhaps more prone to leakage than the 3D printed higher frequency coupler.

The amplitudes for the forward and reverse coupled ports of the large coupler can be seen in Figure 6.8, the forward amplitude follows approximatively the frequency response curve of the loud speaker.

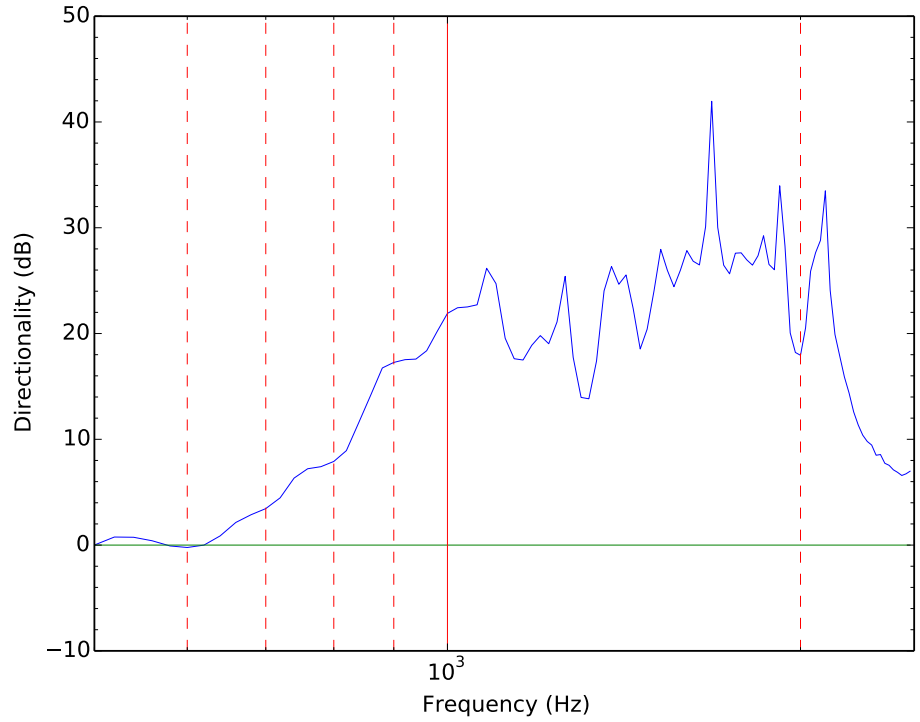

Figure 6.9: The directionality of Pennington's Coupler

The Directionality of the large coupler can be seen in figure 6.9 which we can see is above 20 dB over the designed range, but is much more inconsistent than our 3D printed coupler.

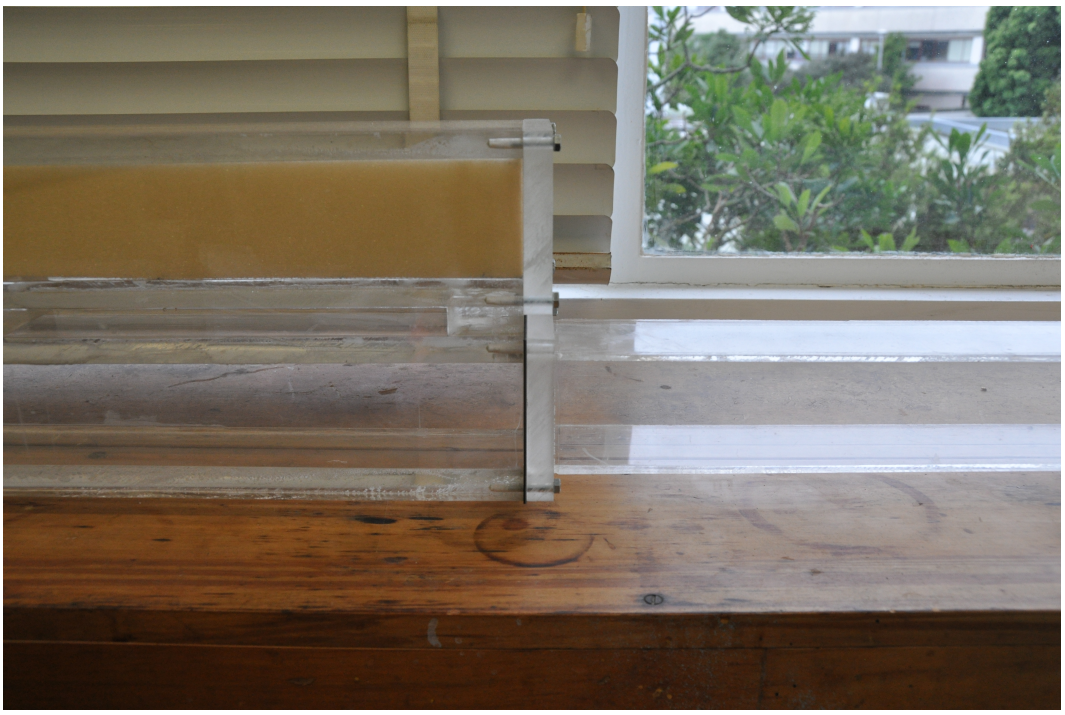

Figure 6.10: Construction of large coupler.

The construction of the large coupler can be seen in Figure 6.10. It is clear that the coupler is built from multiple pieces of plexiglass that are glued together with the end caps bolted to the main body of the coupler. This construction can also be seen in Figure 6.11, here we see the branch lines between the two main lines.

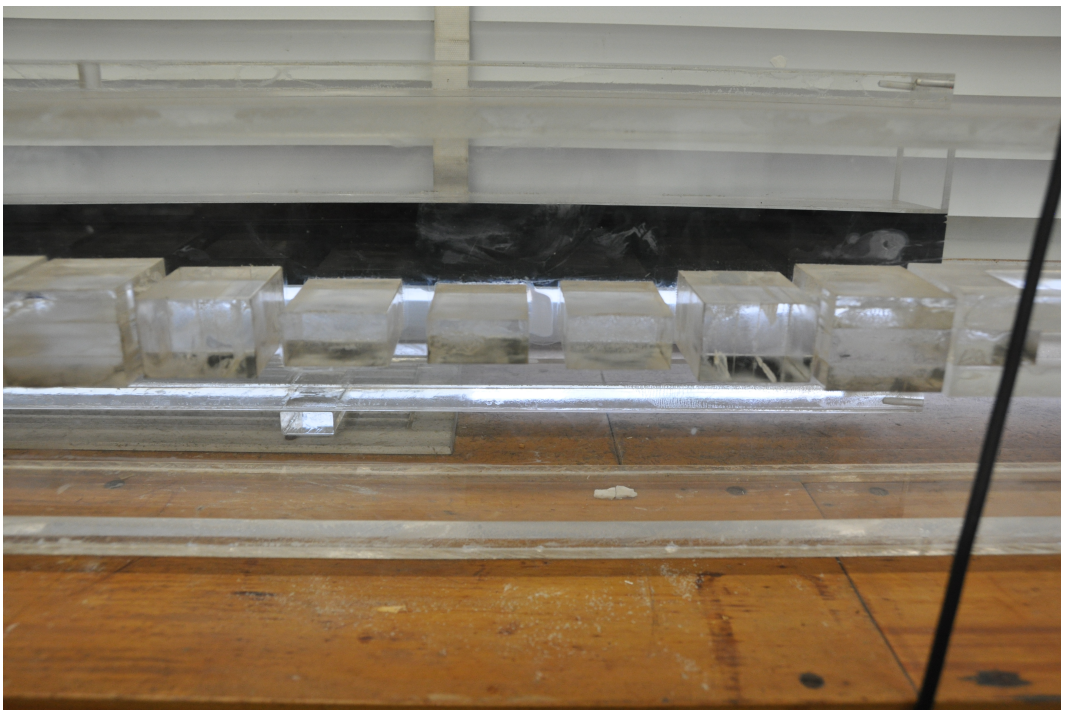

Figure 6.11: Construction of large coupler.

This construction method of gluing and bolting can also be seen in Figure 6.11. Here we can see the branch lines between the two main lines and that the walls separating the mainlines are made using two pieces of plexiglass separated by an air cavity. This construction and thinner walls perhaps contribute to the reduced performance when compared to the Objet30 printed coupler. Interestingly the MakerBot also features air cavities between the walls separating the mainlines, because of the printer material optimization.

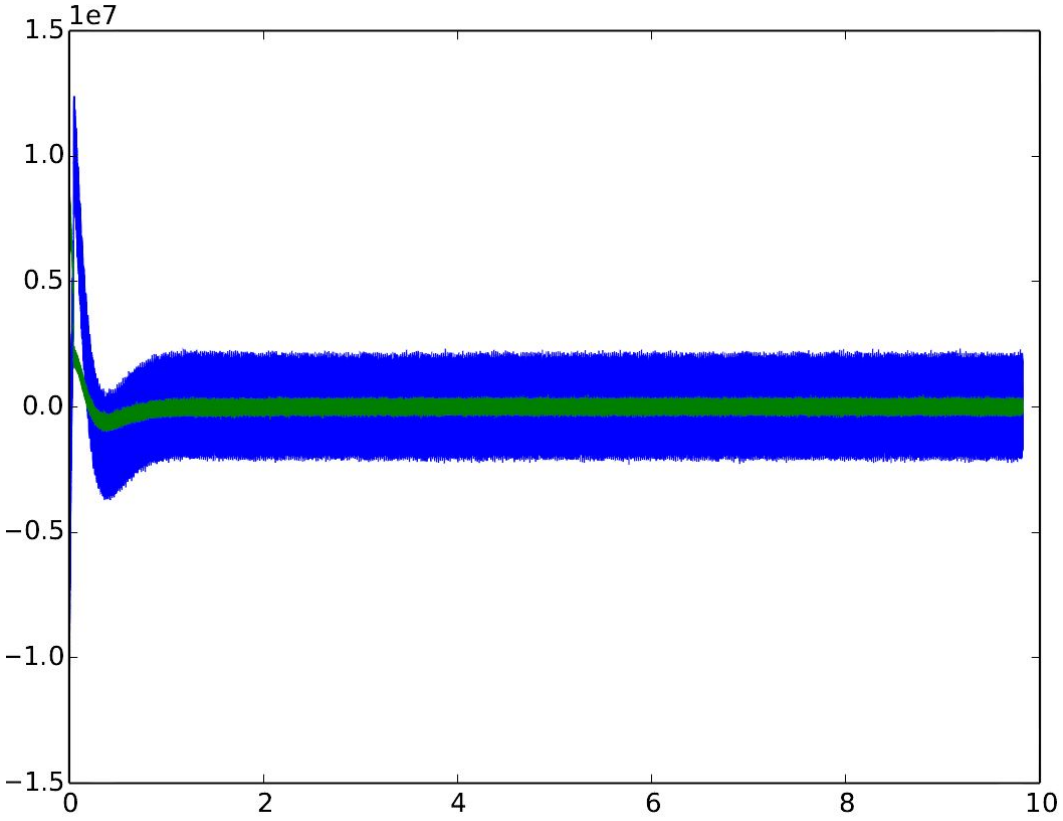

Figure 6.12: Sliding load measurement at 14 kHz, 10 second sample while continuously moving load.

To do an automated measurement of the sliding load test, the file alsa_generate_tones.py was modified and saved as a new script. This script rather than create multiple tones one after another, plays a single tone for a period of ten seconds. While running this script the load slides in a single direction, moved by hand at as constant a rate as possible. In Figure 6.12 the results of this test can be seen. It is difficult to see any change at the scale of figure 6.12. So a zoomed plot was acquired.

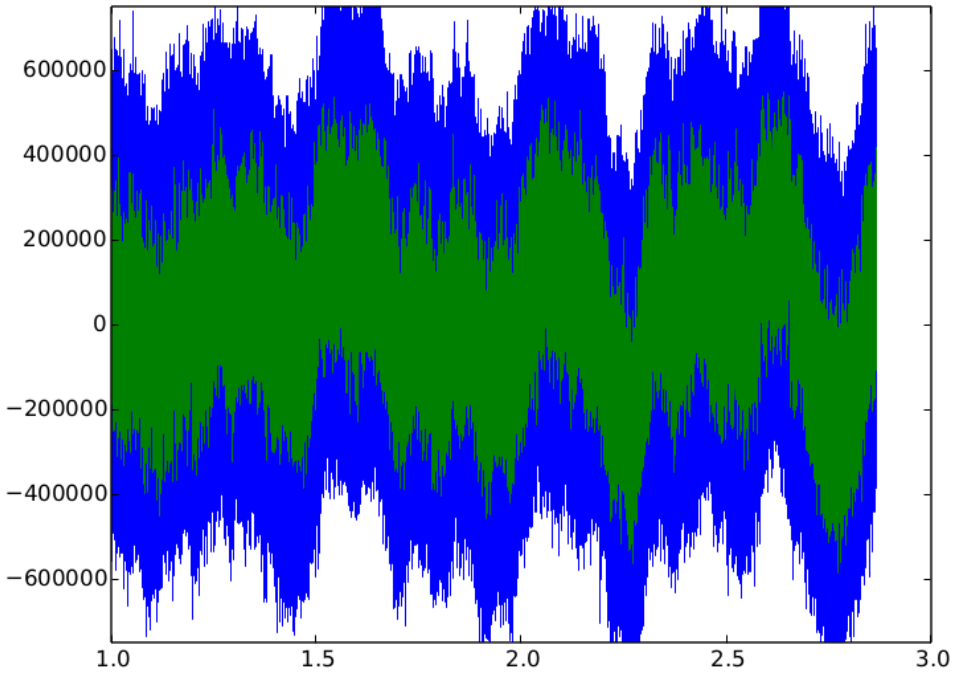

Figure 6.13: Zoomed sliding load measurement at 14 kHz, 10 second sample while continuously moving load.

In the zoomed figure, Figure 6.13 it can be seen that the amplitude of the signal varies. It is unclear if the variation is due to the sliding of the load or low frequency noise. In order to have a definitive indication of load quality a smith chart was required.

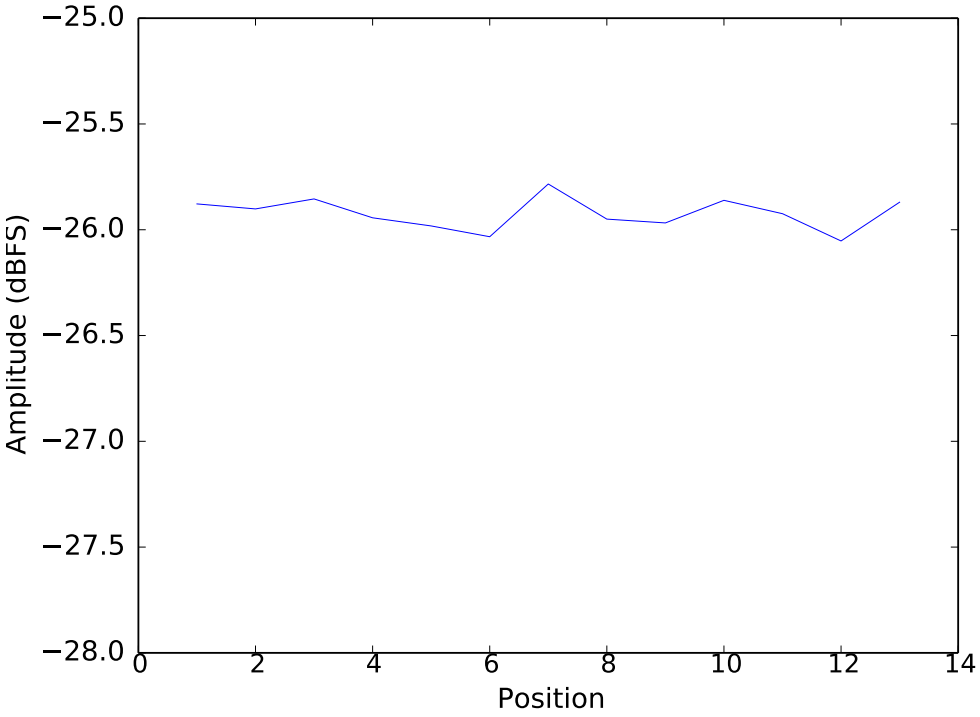

Figure 6.14: Amplitude at coupled port for various load positions.

To create the smith plot, the load is slid to various positions between bursts of signal, the amplitude of the coupled port is measured for the burst and then DFT's are performed to calculate amplitude and phase for each load position at 14 kHz. With each position it can be seen that the amplitude for 14 kHz varies by no more than 0.5 dB. This suggests That our acoustic loads are excellent, agreeing with our initial bench measurement. The low frequency variation seen with load position in 6.13 for a constant 14 kHz tone was noise or unrelated signal.

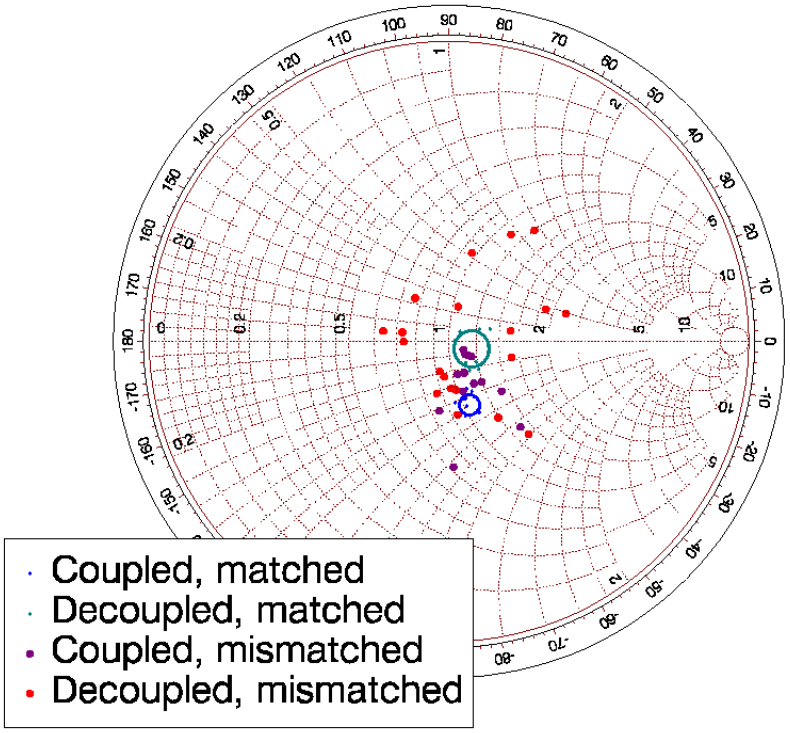

Figure 6.15: Smith chart with fitted circles for the sliding load data both the coupled and decoupled ports using two different loads, a hard plastic load and a foam earplug load.

The smith chart in Figure 6.15 shows data for both a foam earplug load and a hard plastic load. The coupled and decoupled port amplitudes were normalized with the mainline amplitude and plotted as separate data sets. The data for the earplug load at the decoupled port (teal) is indicative of a good load, a tight circle centered very near the center of the smith chart. The coupled port data for the earplug load (blue) forms a tighter blue circle centered some distance from the center of the smith chart.

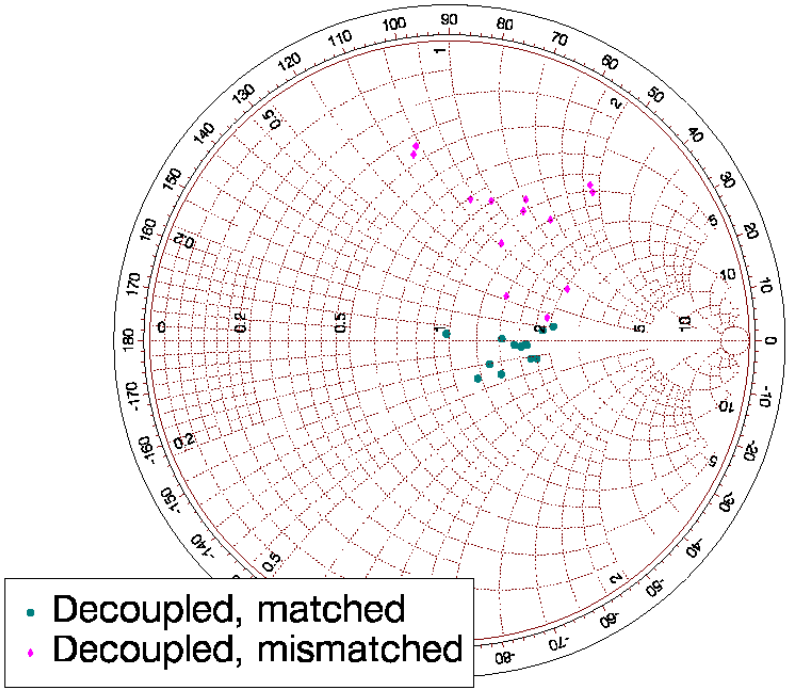

Figure 6.16: Smith chart with for the decoupled port with an input pad, both the hard plastic load and a foam earplug load. The smith chart data scaled by a multiple of 3 (approx 10 dB).

It is difficult to see circles being formed by the data recorded for the hard plastic load (red and purple), but the spread of data would suggest a large fitted circle, this indicates that the hard plastic load is very reflective and far from ideal load. The purpose of the hard plastic load was to offer a comparison between our earplug loads and another material that was expected to perform poorly. The spread in all of the data suggested that our earplug loads were not as good as we had initially hoped, to ensure the spread of data was not due to second order effects a thick foam earplug pad was placed on the input port to stop reflections off of the speaker. The results for the decoupled port with this pad can be seen in figure 6.16, this data was multiplied by 3 (approx 10 dB) so that it could be seen on the smith chart. With the second order effects now minimized we can see that our earplug loads are in fact very good because of such a tight spread in the results (teal), the bad load data (magenta) is seen

to spread more and is indicative of a bad load as we expect.

Chapter 7

Conclusions

7.1 3D printing conclusions

Of the two printers, the Objet30 printer created the superior directional coupler. The MakerBot printed directional coupler suffered from several short comings due to its resolution and printing method. The MakerBot printed coupler had a noticeable grain in its surface finish from the printers crosshatched layering process. There were collapsed portions of mainline waveguide which left the surface finish damaged, and the collapsed plastic had to be cleared from the waveguide before experiments could be started. These collapses were due to the printer not also printing a support structure. The coupler was also warped and shrank by approx 2 mm. This was caused by cooling of the plastic, which affected its overall dimensional accuracy. A second coupler was made using the MakerBot printer for the sake of a physical cross-section. The cross-section revealed that the dimensional accuracy has a potential to distort the branch-guide structure in the coupler so that some walls touch and are not square.

The Objet30 is a comparatively more expensive printer that uses a resin to create the layers of the main structure and also prints a 3D honeycomb wax support structure alternately layer by layer. The support structure of the Objet30 prevents the collapse of the waveguides and the resin layers bond together to give a very smooth surface finish. This surface finish is continued inside the waveguides as a result of the support structure preventing collapse. This printer also creates parts with greater dimensional accuracy because of its resolution and the parts do not warp or shrink as each layer is cured and cooled as it is printed.

The altered characteristics of the MakerBot coupler we believe can be attributed to the decreased resolution of the printer and the absence of a support structure. The resolution perhaps led to not accurately recreating the internal geometry. The absence of a support structure caused the walls of the coupler to collapse. The damaged surface and excess plastic left in the waveguide of the coupler contributing to a change to its behavior.

7.2 Acoustic load and coupler performance conclusions

The oscilloscope traces from the preliminary measurements show that the amplitude at the coupled and decoupled ports were almost completely unchanged by load position. These traces therefore suggested that the foam earplugs would work well as acoustic loads in our coupler.

The directionality measured with the bench equipment for both printed couplers was expected to be better than 20 dB from 10 to 20 kHz, falling away around 7.5 kHz and 22.5 kHz. Both of the measured acoustic couplers displayed excellent directionality, however only the Objet30 version behaved as expected with a range of 7–22 kHz. The Bench measurements suggested that the MakerBot coupler displayed its directionality over a lower frequency band, approximately 7–15 kHz. Because the Objet30 coupler did not suffer any of the issues of the MakerBot coupler from its construction, we attribute its performance to its superior build quality.

The FFT results do not give amplitude to sufficient precision to reliably calculate directionality, therefore we performed DFT's to determine directionality. The DFT calculations resulted in very precise amplitudes Which were processed to give directionality, the Objet30 printed coupler directionality was excellent. The directionality was shown to be essentially a constant 20 dB with frequency, which is far better than we had hoped and predicted with bench measurements. Compared to our bench measurements the directionality calculated using DFT's is calculated as approximately 5 dB better than calculated with the bench measurements on average. The difference is attributed to the inaccuracy of the data collected from the oscilloscope, because of the small scale used without averaging by the oscilloscope to remove noise from traces, human error in reading data from the display was potentially quite large.

The Large low frequency coupler built by Pennington was measured using the same scripts and methods used to measure the 3D printed coupler but

used different microphones powered by the AudioBox phantom power. The directionality measured in this large coupler was less consistent than that of the 3D printed coupler. We attribute this lesser performance to its construction, by being built from multiple parts it is more prone to leakage than the 3D printed coupler. The single piece construction of a 3D printed coupler offers advantages over larger couplers which are assembled from multiple parts because of reduced leakage. The walls separating the mainlines of the large coupler are made using two pieces of plexiglass separated by an air cavity, this construction and thinner walls perhaps contribute to the reduced performance when compared to the Objet30 printer coupler which has very thick walls and no air cavities. Interestingly, the MakerBot also features air cavities between the walls separating the mainlines which may have also contributed to its diminished performance.

When re-testing our foam earplug loads with the automated setup smith charts were created using the data. With an input pad the data for a foam earplug load formed tight circles/groupings which is very convincing evidence of the foam earplugs as a good load material. With an input pad the hard plastic load data was found to produce groupings over a larger area than the foam earplug load. In all the smith chart plots show that foam earplugs are a very good acoustic load material and that hard plastic is a poor acoustic load material.

The results of our investigation firstly indicate that 3D printing is not only an appropriate construction method, but a very effective one. Secondly, scaling a pre-dimensioned coupler has proved to be an effective method for creating couplers with a higher/lower frequency range. Thirdly, has shown that foam earplugs are an effective acoustic load material for the upper half of the audible spectrum.

7.3 Applications, implications and future work

Automated measurement of the MakerBot coupler would have assisted in determining to what extent the Objet30 coupler is superior. Knowing the failings of the MakerBot printer, further 3D design of the SolidWorks model or adjusting printing orientation should be considered to remove and/or minimize undesirable effects from printing by a MakerBot or similar printer. Alterations could potentially see a MakerBot coupler of similar quality to that of the Objet30 coupler. This would greatly reduce the cost of creating small (higher frequency) directional couplers.

The Directional coupler was used as a reflectometer by Lagasse and by Pennington, a reflectometer is a crucial component in a modern vector network analyzer (VNA). Pennington used such a reflectometer to fabricate a single port VNA, The calibration and vector correction techniques used by Pennington could be extended by techniques used in modern electromagnetic VNA's so that in the future a dual-port acoustic VNA could be fabricated. A dual port VNA built using our 3D printed coupler design would benefit from a printed circuit board (PCB) assembly for the MEMS microphones, a more robust seal for the MEMS microphones and a speaker mounting bracket to replace the improvised cardboard harness currently used. Pennington expects his single port VNA to have applications and commercial implications in the fields of architecture, biomedical diagnostics, sound reproduction, and agriculture [4]. It would seem logical that these fields would also thereby benefit from the development of a dual-port acoustic VNA.

In order to create a measurement system that spanned the audible spectrum (20-20,000 Hz), a set of some 10 different-sized couplers would be required. Some applications would benefit from an instrument that reached or exceeded 50 kHz. For an Acoustic coupler to be used in this ultrasound range the coupler would need to be scaled a further 2.5 times. This may potentially prove difficult as the wavelengths at 50 kHz are in the order of mm and comparable with those of electromagnetic waves at 44 GHz.

.1 Appendix1

Listing 1: Python data capture

```
for c in range(5):

  c+=1
  if not os.path.exists("/home/marcus/datadump%d" % c):
      os.makedirs("/home/marcus/datadump%d" % c)

  for freq in [100*x + 700.0 for x in range(990)]:
      count = 0
      print freq
      generator.play(freq, 5, (1*c))
      numpy.set_printoptions(threshold=1000000000)
      # channels = [[],[],[],[],[],[],[],[]]
      data = []

      while generator.is_playing():
          count += 1

          l, raw = inp.read()

          if count > 10000:
              data.extend(numpy.frombuffer(raw, dtype='int32'))


      out_file_name = ("/home/marcus/datadump%d" % c + "/%d" % freq)
      #a=numpy.array(data)
      numpy.save(out_file_name, numpy.array(data))
```

Listing 2: Python Tone Generation and Presonus AudioBox initialization

```
class ToneGenerator(object):

    def __init__(self, samplerate=96000, frames_per_buffer=8820):
        self.p = pyaudio.PyAudio()
        self.samplerate = samplerate
        self.frames_per_buffer = frames_per_buffer
        self.streamOpen = False

    def sinewave(self):
        if self.buffer_offset + self.frames_per_buffer - 1 > self.x_max:
            # We don't need a full buffer or audio so padd the end with 0's
            xs = numpy.arange(self.buffer_offset,
                              self.x_max)
            tmp = self.amplitude * numpy.sin(xs * self.omega)
            out = numpy.append(tmp,
                               numpy.zeros(self.frames_per_buffer - len(tmp)))
        else:
            xs = numpy.arange(self.buffer_offset,
                              self.buffer_offset + self.frames_per_buffer)
            out = self.amplitude * numpy.sin(xs * self.omega)
        self.buffer_offset += self.frames_per_buffer
        return out

    def callback(self, in_data, frame_count, time_info, status):
        if self.buffer_offset < self.x_max:
            data = self.sinewave().astype(numpy.float32)
            return (data.tostring(), pyaudio.paContinue)
        else:
            return (None, pyaudio.paComplete)

    def is_playing(self):
        if self.stream.is_active():
            return True
        else:
            if self.streamOpen:
                self.stream.stop_stream()
                self.stream.close()
                self.streamOpen = False
            return False

    def play(self, frequency, duration, amplitude):
        self.omega = float(frequency) * (math.pi * 2) / self.samplerate
        self.amplitude = amplitude
        self.buffer_offset = 0
        self.streamOpen = True
        self.x_max = math.ceil(self.samplerate * duration) - 1
        self.stream = self.p.open(format=pyaudio.paFloat32,
                                  channels=1,
                                  rate=self.samplerate,
                                  output=True,
                                  frames_per_buffer=self.frames_per_buffer,
                                  stream_callback=self.callback)

inp = alsaaudio.PCM(alsaaudio.PCM_CAPTURE, alsaaudio.PCM_NONBLOCK, )
inp.setchannels(8)
inp.setrate(96000)
inp.setformat(alsaaudio.PCM_FORMAT_S32_LE)
inp.setperiodsize(16)

generator = ToneGenerator()
rubbish = False
```

Listing 3: Python time domain plot, FFT and DFT processing

```
for c in range(1):
        data = []
        period = 1.0/96000.0
        count = 0
        dirlist = []
        dirlist_int = []
        c+=4
        dirlist = os.listdir('/home/marcus/datadump%d' % c)
        for listedfile in dirlist:
                listedfile = re.sub('[!@#$.npy]', '', listedfile)
                listedfile = int(listedfile)
                dirlist_int.append(listedfile)
        dirlist_int = sorted(dirlist_int)
        #print dirlist

        with open('outputdata%d.csv' % c, 'w') as f1:
```

Listing 4: Python time domain plot, FFT and DFT processing; Continued

```
with open('outputdata%d.csv' % c, 'w') as f1:

            for listedfile in dirlist_int:

                    filetoload = ('/home/marcus/datadump%d/' % c + str(listedfile) + '
                        .npy')
                    data = numpy.load(filetoload)
                    times1 = [float(period * y) for y in range(len(data[0::8]))]
                    if not os.path.exists('/home/marcus/plots%d/' % c):
                            os.makedirs('/home/marcus/plots%d/' % c)

                    pp = PdfPages(('/home/marcus/plots%d' % c + '/plot%d.pdf' %
                        listedfile))

                    fig1 = plt.figure()
                    plt.plot(times1, data[0::8], linewidth = 0.2)
                    plt.plot(times1, data[1::8], linewidth = 0.2)
                    plt.xlim(0.05, 0.055)
                    amp1 = data[0::8]
                    amp2 = data[1::8]
                    amp3 = data[2::8]
                    amp4 = data[3::8]
                    pp.savefig()
                    plt.close(fig1)

                    fig2 = plt.figure()
                    n1 = len(data[0::8])
                    n2 = len(data[1::8])
                    mic1fft = numpy.fft.fft(a=data[0::8], n=n1)
                    mic2fft = numpy.fft.fft(a=data[1::8], n=n2)
                    val1 = float(n1 * 1.0/96000.0)
                    val2 = float(n2 * 1.0/96000.0)
                    print val1, val2
                    fftfrequency = numpy.fft.fftfreq(n1, 1.0/96000.0)
                    fft_x_shifted = numpy.fft.fftshift(mic1fft)
                    fft_x_shifted2 = numpy.fft.fftshift(mic2fft)
                    freq_shifted = numpy.fft.fftshift(fftfrequency)
```

Listing 5: Python time domain plot, FFT and DFT processing; Continued

```
                plt.semilogx(freq_shifted, numpy.abs(fft_x_shifted))
                plt.semilogx(freq_shifted, numpy.abs(fft_x_shifted2))
                plt.grid(b=True, which='major', axis='x', color='b', linestyle='-'
                    )
                plt.grid(b=True, which='minor', axis='x', color='r', linestyle='--
                    ')
                plt.yscale('log')
                plt.xlabel("Frequency (Hz)")
                plt.xlim(1000, 100000)
                pp.savefig()
                pp.close()
                plt.close(fig2)
                Output1_tmp = dft.dft([times1[:19999], amp1[:19999]], listedfile,
                    '/home/marcus/tmp/tone')
                Output2_tmp = dft.dft([times1[:19999], amp2[:19999]], listedfile,
                    '/home/marcus/tmp/tone')

                out = ''
                out = str(listedfile)
                out += ','
                out += str(Output1_tmp[1])
                out += ','
                out += str(Output1_tmp[2])
                out += ','
                out += str(Output2_tmp[1])
                out += ','
                out += str(Output2_tmp[2])
                f1.write(out + "\n")
    f1.close()
```

Listing 6: DFT and directionality plot

```
import math
import dft
import sys
import numpy
import re
import os.path
import matplotlib.pyplot as plt
from matplotlib.backends.backend_pdf import PdfPages
channels = []
amp1 = []
amp2 = []
amp3 = []
pp = PdfPages('/home/marcus/plots/DFTplot%d.pdf' % 1)
xs = []
xs1 = []
xs2 = []
xs3 = []
ys1 = []
ys21 = []
ys31 = []
ys2 = []
ys22 = []
ys32 = []
ys3 = []
ys23 = []
ys33 = []
ys4 = []
ys24 = []
ys34 = []
```

Listing 7: DFT and directionality plot; Continued

```
for c in range(4):

        c+=1
        # ratios = []

        with open('outputdata%d.csv' % c, 'r') as f:
                for line in f:
                        line=line.strip()
                        cmpnts = line.split(',')
                        cmpnts = map(float, cmpnts)
                        channels = [0, 1]
                        reference = 1
                        amp = [0, 0]
                        phi = [0, 0]
                        (freq, amp[0], phi[0], amp[1], phi[1]) = cmpnts

                        ratios = []
                        for channel in channels:
                                ratios.append(amp[channel]/amp[reference])
                        # print ratios
                        logs = map(lambda x: 20*(math.log10(x)), ratios)
                        # print c
                        if c==1:
                                xs.append(freq)
                                ys1.append(logs)
                                ys21.append(amp)
                                ys31.append(phi)
                        elif c==2:
                                xs1.append(freq)
                                ys2.append(logs)
                                ys22.append(amp)
                                ys32.append(phi)
                        elif c==3:
                                xs2.append(freq)
                                ys3.append(logs)
                                ys23.append(amp)
                                ys33.append(phi)
                        elif c==4:
                                xs3.append(freq)
                                ys4.append(logs)
                                ys24.append(amp)
                                ys34.append(phi)
```

Listing 8: DFT and directionality plot; Continued

```
plt.autoscale(enable=True, axis=True, tight=True)

fig2 = plt.figure()
for channel, colour in zip(channels, ['b','g']):
        # plt.semilogx(xs, map(lambda x: x[channel], ys21), linewidth = 0.5, color=
            colour)
        plt.semilogx(xs1, map(lambda x: x[channel], ys22), linewidth = 0.5, color=colour
            )
        plt.semilogx(xs2, map(lambda x: x[channel], ys23), linewidth = 0.5, color=colour
            )
        plt.semilogx(xs3, map(lambda x: x[channel], ys24), linewidth = 0.5, color=colour
            )
plt.xlabel('Frequency (Hz)')
plt.ylabel('Amplitude (arb units)')
plt.xlim(7000, 25000)
#plt.ylim(0, 100000)
pp.savefig()


# fig3 = plt.figure()
# for channel, colour in zip(channels, ['b','g']):
#         plt.semilogx(xs, map(lambda x: x[channel], ys3), linewidth = 0.5, color=colour
    )
# plt.xlabel('Frequency (Hz)')
# plt.ylabel('phase')
# plt.xlim(7000, 25000)
# plt.ylim(-180, 180)
# pp.savefig()

fig1 = plt.figure()
for channel, colour in zip(channels, ['b','g']):
        # plt.semilogx(xs, map(lambda x: x[channel], ys1), linewidth = 0.5, color=colour
            )
        plt.semilogx(xs1, map(lambda x: x[channel], ys2), linewidth = 0.5, color=colour)
        plt.semilogx(xs2, map(lambda x: x[channel], ys3), linewidth = 0.5, color=colour)
        plt.semilogx(xs3, map(lambda x: x[channel], ys4), linewidth = 0.5, color=colour)
plt.xlabel('Frequency (Hz)')
plt.ylabel('Directionality (dB)')
#plt.gca().set_yscale('log')
plt.xlim(7000, 25000)
plt.ylim(-10, 35)
pp.savefig()
pp.close()
```

References

[1] ASTM Standard C384, 2004, "Standard test method for impedance and absorption of acoustical materials by impedance tube method".

[2] ISO 10534-1:1996, "Acoustics—determination of sound absorption coefficient and impedance in impedance tubes—Part 1: Method using standing wave ratio".

[3] D. H. Keefe, R. Ling, and J. C. Bulen, "Method to measure acoustic impedance and reflection coefficient", J. Acoust. Soc. Am., vol.91, pp. 470-485, January 1992.

[4] Scott, J. and K. E. Pennington, "Acoustic Vector-Corrected Impedance Meter", *IEEE Transactions on Instrumentation and Measurement, 2014. DOI: 10.1109/TIM.2014.2327474*

[5] Peter D'Antonio, and Brian Rife, "The use of multi-microphone measurements of directional and random incidence acoustical coefficients", Journal of the Acoustical Society of America, April 2012; 131(4):3284.

[6] P.A Rizzi, "Directional Couplers" in Microwave Engineering - Passive Circuits. Englewood Cliffs NJ: Prentice-Hall Inc, 1988, 8, 3, pp 367 - 369.

[7] Lagasse, P., "Realisation of an acoustical directional coupler", Journal of sound and vibration*, 15(3), April 1971, pp367–372.*

[8] "Presonus AudioBox 1818VSL Owners manual" PreSonus Audio Electronics, Inc. 18011 Grand Bay Court, Baton Rouge, LA 70809 USA. pp. 85-86.

[9] Rytting, Doug, "ARFTG 50 year network analyzer history", IEEE MTTS International Microwave Symposium Digest, 2008, pp11-18.

[10] H. C. Heyker, "The Choice of Sliding Load Positions to Improve Network Analyzer Calibration", 12th European Microwave Conference, Helsinki, September 1982, pp429-434.

[11] *L. Brueck, "Assessment of subjective and objective measurement systems of earplug attenuation on an individual", Report for Health and Safety Executive 2013, Harpur Hill Buxton Derbyshire, pp7.*

3D-printed Acoustic Directional Couplers

Marcus MacDonell and Jonathan Scott

***Abstract*—Acoustic Directional Couplers permit separation of forward and reverse sound pressure waves. This separation opens the way to traceable precision acoustic reflection measurements. In order to span the audio frequency range, multiple couplers will be required, as each operates over a frequency range of slightly more than one octave. To reach 20kHz or above requires vary small, mechanically precise construction. We achieve this by 3D printing techniques. We manufactured two otherwise-identical couplers, one made with a powder-type 3D printer with photo-polymer support structure, the other made with an ABS-filament thermoplastic-type 3D printer. We compare the measured acoustic performance of these two couplers. The wavelength of sound at 20 kHz is comparable to that encountered at a microwave frequency of 18 GHz. We expect to be able to fabricate couplers that reach 55 kHz where the wavelength is 6 mm, corresponding to a frequency of 50 GHz in the electromagnetic spectrum.**

***Index Terms*—Acoustical engineering, acoustic measurements, acoustic devices, directional couplers, waveguides**

I. Introduction

A Directional Coupler is a 4-port network in which portions of the forward and reverse traveling waves on a transmission line are separately coupled to two of the ports [1]. It is often assumed that a directional coupler is inherently an electromagnetic device, since the majority of commercial examples have either coaxial or electromagnetic waveguide ports. Nevertheless, acoustic directional couplers also exist. These are four port devices and behave much like a conventional directional coupler, except that the ports are acoustic waveguides that conduct pressure waves in a medium, typically air. A design for an acoustic directional coupler is described in [2]. For an acoustic coupler the required coupler material thickness is a non-negligible fraction of the wavelength and needs to be sufficiently stiff. Because of this a branch coupler is the most suitable design. A Branch coupler uses short sections of waveguide to couple the two mainlines. [2] Using a branch coupler also has an advantage, the thickness of the separating wall not only contributes to the isolation of the two mainlines but also improves the performance of the network. [2]

The Coupler can be used as a reflectometer to make extremely accurate measurements of a materials acoustic properties. These measurements can be used by the audio industry to better isolate recording studios, damp speaker cabinets, design concert halls and theaters. Vector correction techniques will allow a user to correct for all shortcomings of a coupler provided the directivity of the coupler is sufficient (usually better than 6–10 dB). [3]

The directionality of a coupler is thus the most important specification, and is the specification we are most concerned with for determining the performance of the acoustic directional coupler. The directionality or directivity is defined as $10log(P_c/P_d)$ where P_c is the power at the coupled port and P_d is the power at the decoupled port [1].

Recently a version of the Lagasse design has been used to fabricate an acoustic impedance meter [3]. The coupler used 60 mm-square waveguide and had a design frequency range of 1–2 kHz and a usable range of 800–2,200 Hz.[1] It was constructed by welding sheets and machined blocks of acrylic material. In [3] it was shown that vector correction allowed precise measurements of acoustic S-parameters. In order to create a measurement system that spans the audio range from 20-20,000 Hz a set of some 10 different-sized couplers would be required. Some applications would benefit from an instrument that reached or exceeded 50 kHz.

We created a SolidWorks model of the Lagasse coupler design. Once established, this design can be scaled, as dimensions scale inversely with operating frequency. We built two versions, 3D-printed on different printers. The first was a MakerBot Replicator 2X that employs an ABS filament material. It claims a layer resolution of 200 microns [0.0078 inches], and am X-Y resolution of 11 microns. The second was an Objet30 Pro powder-type 3D printer with photo-polymer support. This machine claims a layer thickness of 28 microns and a resolution of 100 microns [0.0039 inches].

We wish to determine if there is a minimum 3D printer resolution to maintain directionality or if the resolution has a considerable effect on directionality for the chosen operational frequency.

There is very little literature concerning the use, design and application of acoustic directional couplers. The original paper by Lagasse, [2], seems to have been largely ignored. In [3] the authors describe a number of systems in the literature that discrimate travelling waves, but all others use alternatives apart from directional couplers. The literature surrounding the use of electromagnetic couplers is very rich, in contrast. [1], [4]

II. SolidWorks model and Construction

The acoustic directional coupler model was designed to operate in a frequency range an order of magnitude higher than that of the hand-built coupler from [3]. The designed frequency range therefore is 10–20 kHz.

Figure 1 shows a block diagram of the coupler in use. A loudspeaker followed by a small pad introduces signal into port one. A matched load absorbs energy on port two. Ports 3 and 4 also have matching loads but each also has a microphone to sample the signal going into the side load.

The authors are with the School of Engineering, the University of Waikato, Hamilton, New Zealand. e-mail: jonathanscott@ieee.org

[1]It should be noted that while rectangular electromagnetic waveguides have a theoretical lower cutoff frequency, acoustic waveguides do not. For this reason an acoustic waveguide will theoretically work all the way from DC to the frequency at which multimoding is possible. In practice, the air-tightness will introduce a rolloff below some frequency. The upshot is that the operating bandwidth has the potential to be larger than 1 octive.

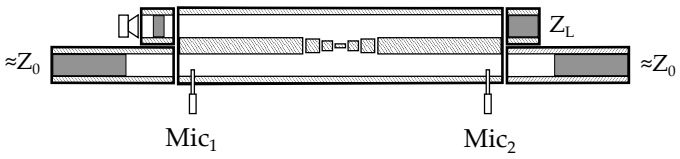

Fig. 1. "Block diagram of the acoustic hardware. Microphones sense the sound pressure level in the two side arms of the coupler. The source is a small loudspeaker mounted behind an attenuating pad constructed of the same foam rubber used to make the loads" [3].

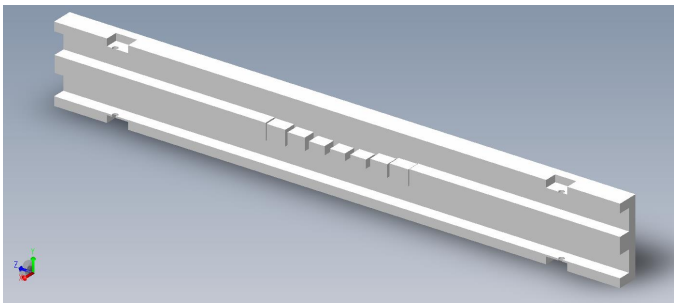

Fig. 2. SolidWorks model for the acoustic directional coupler.

In the SolidWorks model there are side-ports for the placement of MEMS (Micro-Electro-Mechanical Systems) microphones. The cross section view in Figure 2 also allows us to see the internal geometry which is responsible for the directionality of the coupler. The Block diagram shows loudspeaker and load placement.

The ABS filament type MakeBot created a Coupler with a noticeable grain from its crosshatched layering process. More importantly it also had collapsed portions in the waveguide. The collapsed portions left the surface finish damaged and the collapsed plastic had to be cleared before experiments could be started. The Coupler is also slightly warped from the cooling of the layers of plastic which affects its overall dimensional accuracy. These defects can be seen in Figures 3, 4 and 5.

Fig. 3. MakeBot coupler surface finish (Top) and collapsed plastic (Bottom Left).

The Objet30 is printed with a support structure. The wanted structure and removable support layers are printed alternately layer by layer. The support structure makes a significant difference to the finish of the coupler as well as its dimensional accuracy. The support structure is removed with a dilute sodium hydroxide solution.

Fig. 4. Another MakeBot coupler, cross section: Cut with a band saw, poor surface finish can be seen on the roof of the coupler (upper half in the photo).

Fig. 5. MakeBot coupler cross section: At this angle inacurracy in the internal geometry can be seen, the most extreme left and right wave guide portions are deformed and almost touching at points. The seperation should be 0.276 mm or 276 microns.

III. Measurements

We seek to measure the directionality of the coupler samples. Referring to figure 1, we hope that signal originating from the loudspeaker on port 1 will be mostly passed to port 2 (top right-hand port in the figure) and there absorbed by the load Z_L, if it is a good match to the characteristic impedance Z_0. A small proportion of the loudspeaker signal should be coupled to port 3 where it is sampled by Mic 2 and absorbed by the load in that arm of the coupler. If no signal is reflected from the load on port 2, no signal should be detected on the isolated port, port 4, sampled by Mic 1. The directionality of the coupler, in this case, will be the ratio of signals at Mic 1 to those at Mic 2. This directionality is ideally infinite. In practice we expect values in the range 10–40dB for realisable designs.

The measurement of directionality depends upon the quality of the loads used at ports 2–4. For example, if the load port,

port 2, is terminated in a perfect reflection instead of a perfect load, the directinality will disappear completely as the signals in the two microponoes will ideally be the same. How then can we know that our measurement is reasonably reliable, that is that the measurement of directionality has not been compromised by non-ideality of the terminating loads? We gauge the quality of the terminating load by sliding it along the guide. This has the effect of changing the phase of any reflected component. As the phase changes, the magnitudes at the microphones are observed. If there is a significant component changing phase, there will be a significant change in measured signal amplitude. We observe very little. We believe that our terminations, visible in figure 6, reflect below -20dB of incident signal, and often -40dB.

In fact, we chose the material used as the loads by means of this sliding load method from [3]. It was found that generic yellow earplugs worked relatively well.

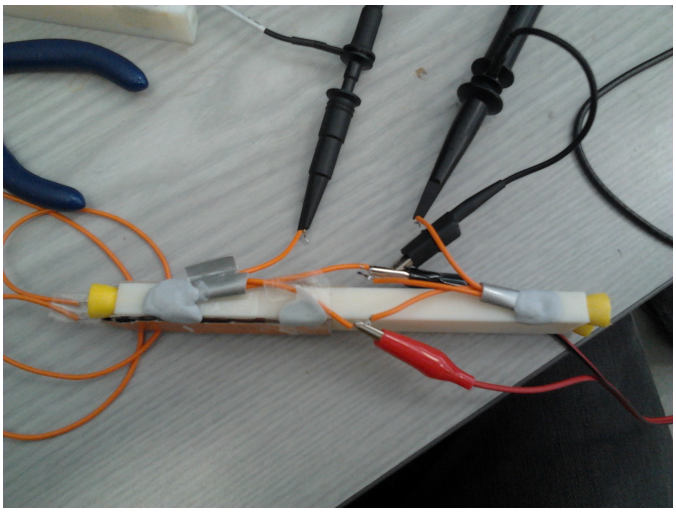

Fig. 6. Coupler experimental set up. Earplugs can be seen as the yellow foam inserted at the ends. Microphones are sealed into the top of the coupler with Blutack™

For our experiments to measure directionality yellow earplugs were used as acoustic loads on three of the coupler's four ports. Measurements were made using an Agilent 33220A function generator into a Digitech stereo amplifier which powered a small diaphragm transducer on the input of the coupler. Two MEMS microphones attached to the coupler were used to detect the tone amplitude through a Tektronix TDS2014C oscilloscope. The MEMS microphones are powered at 3 V from a bench power supply. The experimental set up can be seen in Figure 6. All measurements were done by hand. It is hoped that there will be automated measurements shortly.

A. MakeBot Acoustic Coupler

In order to test the coupler we put a swept audio signal into port one with a matched load on port two. Ideally we would see a strong signal on the coupled port and a much smaller signal on the decoupled port. Figure 7 shows the result of the measurement. The amplitudes in the MakeBot acoustic coupler were measured as voltage signals from the microphones. We are most interested in the ratio of the coupled to decoupled port signals, the directivity of the coupler. Directivity is plotted in figure 8. Directivity is expected to be better than 20 dB from 10 kHz to 20 kHz, falling away around 7.5 kHz and 22.5 kHz. Directivity is excellent from below 10 kHz to at least 15 kHz, but it appears as if the expected characteristic has been shifted towards lower frequencies. The MakeBot coupler demonstrated apparently excellent performance but not over the expected frequency range. The directionality was better than 15 dB from 6 kHz to 15 kHz, but disappeared completely at around 18 kHz. (The transducer prevented measurement at lower frequencies.) We attribute this unexpected performance to the mechanical imperfections of the printing process, and we believe the extended low-frequency performance is a coincidence upon which it will not be possible to rely.

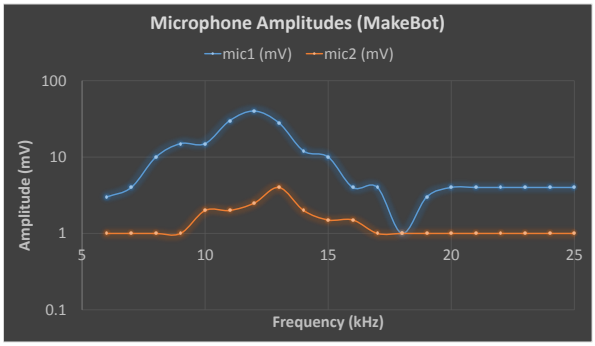

Fig. 7. The lower resolution print port amplitudes.

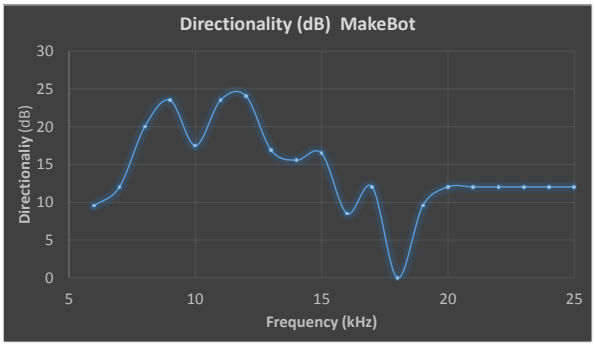

Fig. 8. The lower resolution print directionality.

B. Objet30 Acoustic Coupler

Using the same method the amplitudes on the coupled and decoupled ports of the Objet30 coupler were measured. Directivity is again expected to be better than 20dB from 10 to 20 kHz. Figures 9 shows the directionality for the Objet30

Coupler. The Directivity for the Objet30 coupler is excellent and extends outside the designed range. The Directivity extends over a range of 7–22 kHz.

We believe the low frequency extension below 7 kHz is unreliable as the signal is heavily attenuated, approaching the noise floor. The Objet30 coupler behaves as expected and we attribute this to the increased resolution and accuracy of the printer due to its support structure stopping any collapsing during printing.

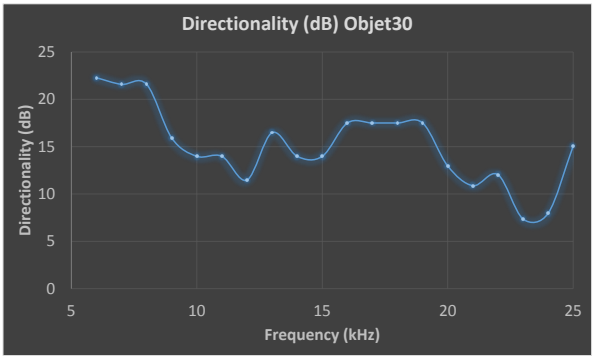

Fig. 9. Acoustic coupler directionality averages 15 dB over the expected usable frequency range.

IV. Conclusion

Directivity for both printed couplers was expected to be better than 20dB from 10 to 20 kHz, falling away around 7.5 kHz and 22.5 kHz. Both of the measured acoustic couplers displayed excellent directionality. However only the Objet30 version behaved as expected with a range of 7–22 kHz. The MakeBot coupler displayed its directivity over a lower frequency band, approximately 7–15 kHz.

The altered characteristics of the MakeBot coupler we believe can be attributed to the decreased resolution of the printer and the absence of a support structure. The internal geometry of the MakeBot coupler was inaccurate due to the lower resolution and absence of support structure. The absence of a support structure caused the walls of the coupler to collapse. These features and the damaged surface and excess plastic left in the waveguide of the coupler caused a change to its behavior.

The Objet30 coupler did not suffer any of these issues from its construction and we attribute its performance to its superior build quality.

References

[1] P.A Rizzi, "Directional Couplers" in *Microwave Engineering - Passive Circuits.* Englewood Cliffs NJ: Prentice-Hall Inc, 1988, 8, 3, pp 367 - 369.

[2] Lagasse, P., "Realisation of an acoustical directional coupler", *Journal of sound and vibration*, 15(3), April 1971, pp367–372.

[3] Scott, J. and K. E. Pennington, "Acoustic Vector-Corrected Impedance Meter", *IEEE Transactions on Instrumentation and Measurement, 2014. DOI: 10.1109/TIM.2014.2327474*

[4] Rytting, Doug, "ARFTG 50 year network analyzer history", IEEE MTT-S International Microwave Symposium Digest*, 2008, pp11–18.*

[5] ISO 10534-1:1996, "Acoustics—determination of sound absorption coefficient and impedance in impedance tubes—Part 1: Method using standing wave ratio".

[6] ASTM Standard C384, 2004, "Standard test method for impedance and absorption of acoustical materials by impedance tube method".

FRONT PANEL :- TEKTRONIX TDS2024 OSCILLOSCOPE.

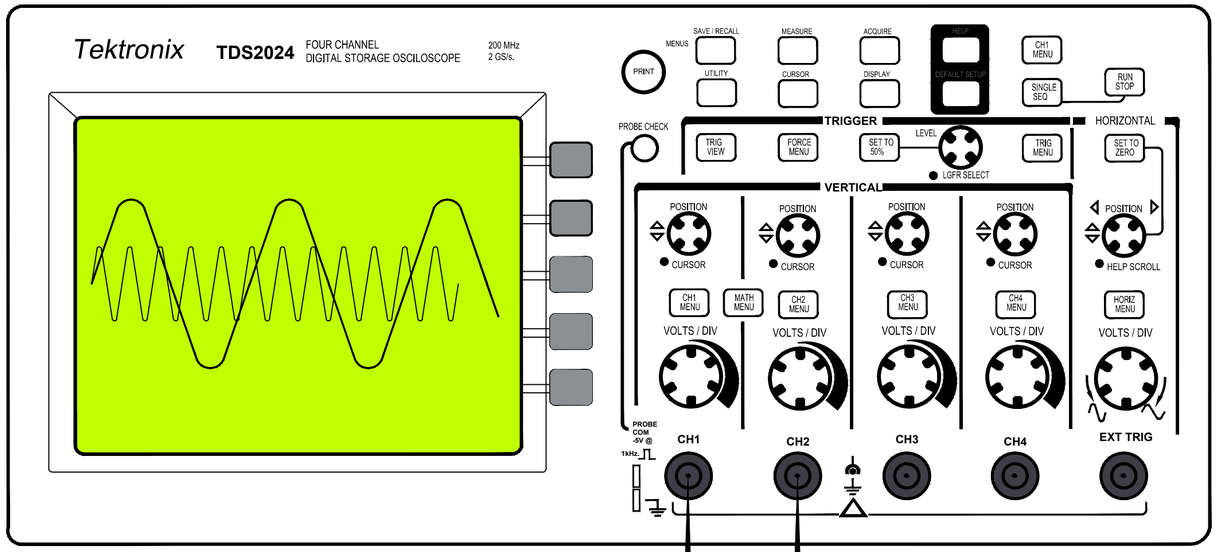

FRONT PANEL :- SIGNAL GENERATOR.

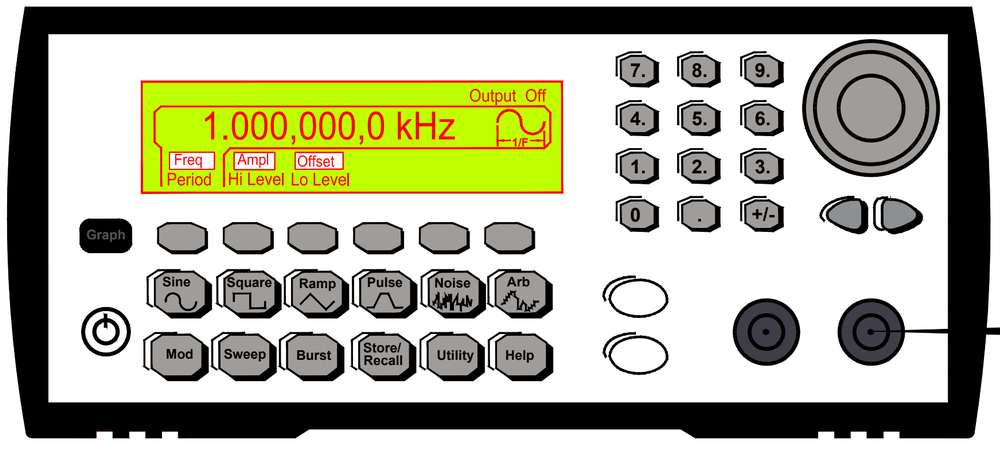

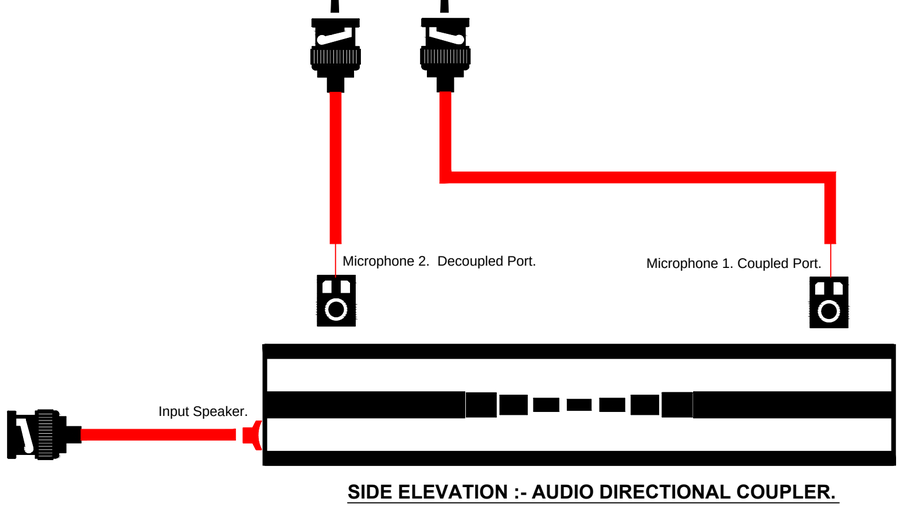

SIDE ELEVATION :- AUDIO DIRECTIONAL COUPLER.

SCHEMATIC DIAGRAM OF THE INITIAL MANUAL BENCH SETUP

NOTES SPECIAL TO ILLISTRATION :-

1. All connections and hardware shown in the schematic diagram with the exception of a benchtop power supply to power up the MEMS (Micro electro-mechanical systems) microphones.

ILLUSTRATION CONCEPT AND PROCESS INFORMATION.	
STUDENT	M.S.G. MacDONELL
SUPERVISING PROFESSOR	J.B.SCOTT
ILLISTRATOR	S.G. MacDONELL
SUBMISSION DATE	MAY 2015.
SCALE:	N.T.S.

KO TE TANGATA

UNIVERSITY OF WAIKATO
SCHOOL OF ENGINEERING

A2 DRAWING SHEET AS AN ATTACHMENT TO A THESIS SUBMITTED. IN FULFILMENT OF THE REQUIREMENTS FOR THE DEGREE OF MASTER OF ENGINEERING (ELECTRONICS) AT THE UNIVERSITY OF WAIKATO

THESIS TOPIC	SCALING ACOUSTIC DIRECTIONAL COUPLERS USING 3D PRINTERS.	
DETAILS SHOWN ON DRAWING	SCHEMATIC DIAGRAM OF THE INITIAL MANUAL BENCH SET UP.	A2 DRAWING ATTACHMENT SHEET
		SHEET 1 OF 2

A2

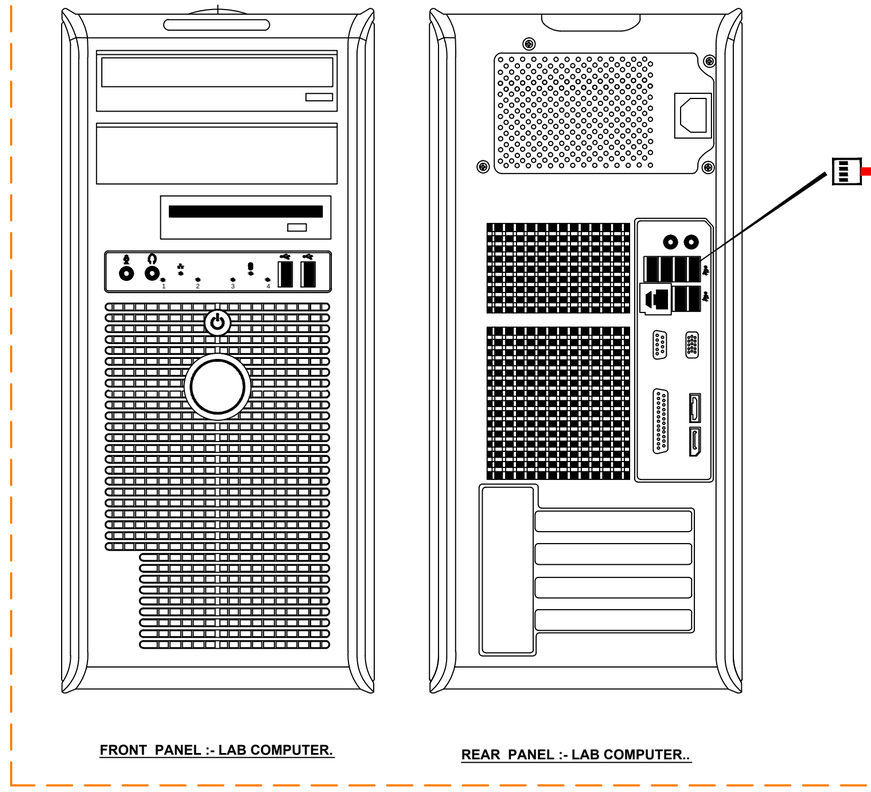

FRONT PANEL :- LAB COMPUTER.

REAR PANEL :- LAB COMPUTER..

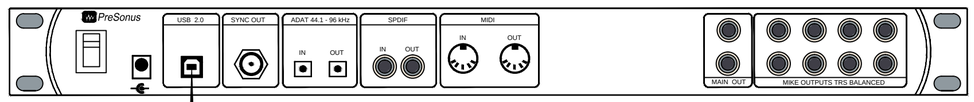

REAR PANEL :- PRESONUS AUDIOBOX 1818VSL.

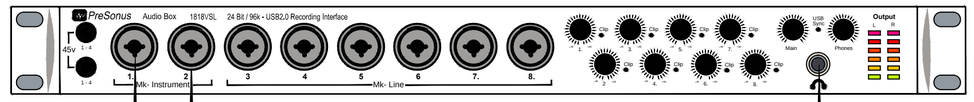

FRONT PANEL :- PRESONUS AUDIOBOX 1818VSL.

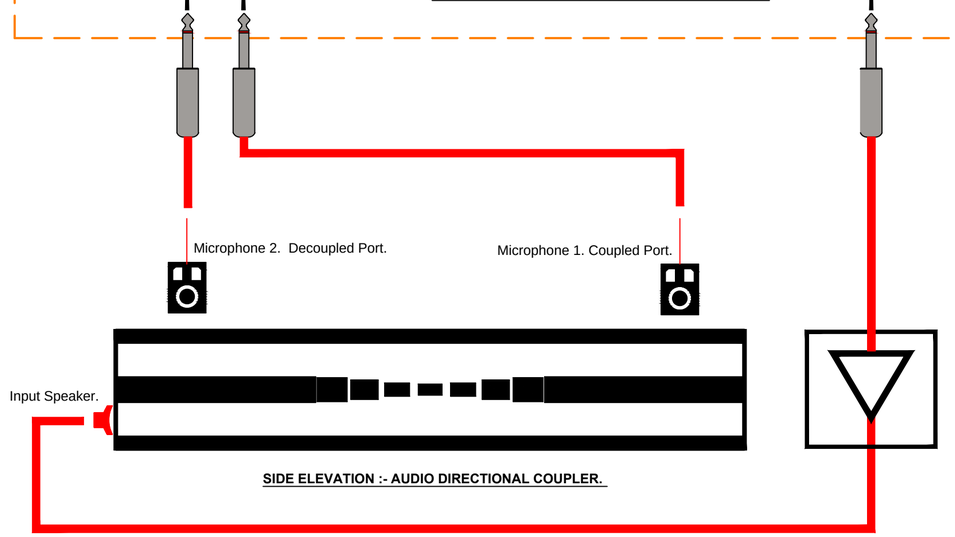

SIDE ELEVATION :- AUDIO DIRECTIONAL COUPLER.

SCHEMATIC DIAGRAM OF AUTOMATED COUPLER TEST SET .

NOTES SPECIAL TO ILLISTRATION :-

1. All connections and hardware shown in the schematic diagram with the exception of a benchtop power supply to power up the MEMS (Micro electro-mechanical systems) microphones.

ILLUSTRATION CONCEPT AND PROCESS INFORMATION.	
STUDENT	M.S.G. MacDONELL
SUPERVISING PROFESSOR	J.B.SCOTT
ILLISTRATOR	S.G. MacDONELL
SUBMISSION DATE	MAY 2015.
SCALE:	N.T.S.

KO TE TANGATA

UNIVERSITY OF WAIKATO
SCHOOL OF ENGINEERING

A2 DRAWING SHEET AS AN ATTACHMENT TO A THESIS SUBMITTED. IN FULFILMENT OF THE REQUIREMENTS FOR THE DEGREE OF MASTER OF ENGINEERING (ELECTRONICS) AT THE UNIVERSITY OF WAIKATO

THESIS TOPIC	SCALING ACOUSTIC DIRECTIONAL COUPLERS USING 3D PRINTERS.	
DETAILS SHOWN ON DRAWING	SCHEMATIC DIAGRAM OF AUTOMATED ACOUSTIC COUPLER TEST SET	A2 DRAWING ATTACHMENT SHEET
		SHEET 2 OF 2

A2